Available online at www.sciencedirect.com

SCIENCE DIRECT

Developmental Biology 277 (2005) 296–315

DEVELOPMENTAL BIOLOGY

www.elsevier.com/locate/ydbio

Olfactory and lens placode formation is controlled by the hedgehog-interacting protein (*Xhip*) in *Xenopus*

Yvonne Cornesse, Tomas Pieler, Thomas Hollemann*,[1]

Department of Developmental Biochemistry, Institute of Biochemistry and Molecular Cell Biology, Georg-August-University of Göttingen, D-37077 Göttingen, Germany

Received for publication 8 March 2004, revised 8 September 2004, accepted 9 September 2004
Available online 26 October 2004

Abstract

The integration of multiple signaling pathways is a key issue in several aspects of embryonic development. In this context, extracellular inhibitors of secreted growth factors play an important role, which is to antagonize specifically the activity of the corresponding signaling molecule. We provide evidence that the *Hedgehog-interacting protein* (*Hip*) from *Xenopus*, previously described as a Hedgehog-specific antagonist in the mouse, interferes with Wnt-8 and eFgf/Fgf-8 signaling pathways as well. To address the function of Hip during early embryonic development, we performed gain- and loss-of-function studies in the frog. Overexpression of *Xhip* or *mHip1* resulted in a dramatic increase of retinal structures and larger olfactory placodes primarily at the expense of other brain tissues. Furthermore, loss of *Xhip* function resulted in a suppression of olfactory and lens placode formation. Therefore, the localized expression of *Xhip* may counteract certain overlapping signaling activities, which inhibit the induction of distinct sensory placodes.

Keywords: Hh; Fgf; Wnt; Hip; Retina; Lens; Placode; Olfactory; *Xenopus laevis*

Introduction

Fate mapping studies and the use of molecular markers have shown that the visual system of vertebrates originates from cells located within the anterior neural plate (Eagleson and Harris, 1990; Eagleson et al., 1995; Vogt, 1929; Zuber et al., 2003). The first morphological sign of vertebrate eye development is the appearance of mirror-imaged evaginations on both sides of the ventro-lateral diencephalon, referred to as eye vesicles. The two eye vesicles grow distally until they reach the surface ectoderm on either side of the embryo. The remaining connections between the brain and the eye vesicles will later form the optic stalks. The contact between the surface ectoderm and eye vesicles induces lens placode formation within the surface ectoderm and vice versa, signals from the lens placodes provide information for proper patterning of the retina (Ashery-Padan et al., 2000; Mangold, 1931; Twitty, 1930; Zygar et al., 1998). The most distal area of the eye vesicle invaginates and contributes to the inner neural layer of the retina. More proximally located cells of the eye vesicle develop into the outer layer of the retina, which gives rise to the non-neural retinal pigment epithelium (RPE). During this process, the lens vesicle is embedded into the optic cup, and together these form the embryonic eye (Chow and Lang, 2001; Saha et al., 1992; Wawersik and Maas, 2000).

The lens placode belongs to a series of regional thickenings of the ectoderm from which a multitude of elements of the sensory neural system originate during vertebrate development (Schlosser and Northcutt, 2000). Cell lineage and grafting studies in amphibian and chicken embryos have provided evidence that these cranial placodes include, for example, parts of the otic anlagen, cranial

* Corresponding author. Department of Developmental Biochemistry, Institute of Biochemistry and Molecular Cell Biology, Georg-August-University of Göttingen, Justus-von-Liebig-Weg 11, D-37077 Göttingen, Germany. Fax: +49 551 5573811.
E-mail address: thomas.hollemann@medizin.uni-halle.de (T. Hollemann).
[1] Present address: Institute of Physiological Chemistry, Martin-Luther-University Halle-Wittenberg, Hollystraße 1, D-06114 Halle (Saale), Germany.

0012-1606/$ - see front matter © 2004 Elsevier Inc. All rights reserved.
doi:10.1016/j.ydbio.2004.09.016

nerves, the lens, and the olfactory anlage. There they give rise to a variety of cell types, like peripheral neurons as well as to other non-epidermal cell types. During gastrulation, the sensory placodes develop from a common territory, which appears as a stripe adjacent to the border of the anterior neural plate and is referred to as the preplacodal ectoderm field. During further development, the competence of a given placodal subpopulation to respond to instructive signals becomes more and more defined and is finally restricted to a specific fate (Baker and Bronner-Fraser, 2001; Grainger, 1992; Reiss and Burd, 1997; Schlosser and Ahrens, 2004).

A large number of genes and mutations identified in the past years are involved in the process of eye and placode development, but relatively little is known of how their expression is controlled. These factors include transcriptional regulators, like Otx2 (Pannese et al., 1995), Pax6 (Hirsch and Harris, 1997), Six3 (Oliver et al., 1995; Zhou et al., 2000), and Xtll (Hollemann et al., 1998), which are expressed in prospective lens, olfactory, and retinal ectoderm, while others are restricted to the prospective lens ectoderm, like Pitx1 (Hollemann and Pieler, 1999) and Lens1 (Kenyon et al., 1999), or as for Rx1 (Mathers et al., 1997), in prospective retinal ectoderm. Subsequently, a multitude of transcription factors, such as Pitx3 (Pommereit et al., 2001), MafA, and MafB (Ishibashi and Yasuda, 2001), participate specifically in the determination of the lens fate, whereas others, such as Chx10 (Liu et al., 1994), Rx2 (Chuang et al., 1999), and Six6 (Bernier et al., 2000; Zuber et al., 1999), are essential for retinal cell differentiation. In addition, secreted signaling molecules, like BMPs (Furuta and Hogan, 1998; Wawersik et al., 1999), FGFs (Hyer et al., 1998; McAvoy et al., 1991; Zhao et al., 2001), Hedgehog proteins (Amato et al., 2004), and retinoic acid (Enwright and Grainger, 2000; Hyatt et al., 1996; McCaffery and Drager, 1993) are present within the developing eye. Wnt antagonists, such as sFrp1/2 (Hyatt et al., 1996; Ladher et al., 2000), are also involved in multiple aspects of eye and placode development (Chow and Lang, 2001). With the exception of Pitx1 and Lens1, a similar set of genes is involved in the early development of the olfactory placode. Here, Dlx5, and Emx2 are involved in the specification of the olfactory fate (Long et al., 2003; Pannese et al., 1998).

Eye development and placode induction are closely linked to neural development, which is mediated through the inhibition of BMP signals by secreted antagonists, such as noggin, chordin, follistatin, and cerberus, and is regarded as the default state of ectoderm (Munoz-Sanjuan and Brivanlou, 2002; Wessely and De Robertis, 2002). In the chick, it has been reported that the inhibition of BMP signaling is needed for the maintenance rather than for the initial induction of neural fate. Here, Fgf and/or inhibitors of Wnt signals act earlier than BMP signals on ectodermal cells to specify neural precursors. While Fgf attenuates BMP activity (Pera et al., 2003), late Wnt signals have been found to suppress the activity of Fgf (Streit et al., 2000; Wilson et al., 2001). In *Xenopus*, early Wnt/β-catenin signals antagonize *Bmp4* gene activity (Baker et al., 1999; Wessely et al., 2001) and a Wnt target gene, *Xiro1*, negatively regulates *Bmp4* expression (Gomez-Skarmeta et al., 2001). Nevertheless, early neural precursor cells can still respond to a non-neuralizing signal, such as BMP4, which induces an epidermal fate. Thus, BMP antagonists might prevent the suppression of an earlier specified neural fate (Harland, 2000).

Although pattern formation of the posterior neural plate has been studied in detail (Briscoe et al., 2000; Marquardt and Pfaff, 2001), less is known about the molecular mechanisms underlying early regionalization of the prospective head region and the corresponding placodal ectoderm (Crossley et al., 2001; Rubenstein et al., 1998). One key event is the establishment of certain organizing centers from which permissive and/or instructive signals emerge. Two main signaling centers within the anterior neural plate have been described, the anterior neural ridge (ANR) and the border between midbrain and hindbrain (MHB), which both express different Fgfs and Wnts as well as other factors to pattern the prospective head region in an anterior–posterior direction (Lekven et al., 2003; Ohkubo et al., 2002; Wurst and Bally-Cuif, 2001). In addition, patterning of the anterior neural plate along the medial–lateral axes is under control of the midline-secreted glycoprotein Sonic Hedgehog (Ingham and McMahon, 2001). Furthermore, lateral patterning is regulated by BMPs emanating from adjacent non-neural ectoderm and BMP function is required for sensory placode formation (Pera et al., 1999; Wawersik et al., 1999; Woda et al., 2003). Therefore, certain overlapping signaling activities within the area between neural plate and non-neural ectoderm seem to synergize in the induction of the neural crest territory and in the definition of distinct sensory placodes.

In this report, we describe the cloning and functional characterization of the hedgehog-interacting protein from *Xenopus* (*Xhip*), which we also found to interfere with the eFgf/Fgf-8 and Wnt-8 pathways in addition to its interference with Hh signaling. Hip was originally identified as an Hh-interacting protein in mice, which binds to and therefore attenuates the activity of secreted Hh (Chuang and McMahon, 1999). Recently, it was reported that the targeted disruption of the *Hip1* locus in mice impaired lung branching morphogenesis and led to a delayed mineralization in mutant skeletons, which was explained by an up-regulation of Hh signaling (Chuang et al., 2003). Previously, we reported that *mHip1* overexpression in *Xenopus* embryos, along with other Hedgehog-inhibitors, resulted in the induction of enlarged or ectopic otic vesicles (Koebernick et al., 2003). Here, we show that *mHip1* overexpression additionally led to an enormous increase of eye-like structures and enlarged olfactory placodes, similar to what has been reported for the repression of Wnt and Fgf signals (Glinka et al., 1997; McGrew et al., 1997). Loss of *Xhip* function by antisense morpholino microinjection resulted in a specific suppression of olfactory placode and lens formation, which in the latter case also impaired proper retina formation.

Materials and methods

Cloning of Xenopus Hip and RT-PCR analysis

A 333-bp cDNA fragment of *Xenopus Hip* was amplified by RT-PCR from stage 26 RNA preparations using degenerate primers (Fdeg-GGAGAYGAAAGRGGMYTGCTAAGCC; Rdeg-CCTGTGAARTCACTYARMCCATCCAT). Homologous primers were generated to screen a λ-ZAP express cDNA library prepared from isolated heads of stage 32 *Xenopus* embryos (Hollemann et al., 1998). One positive pool was plated and screened by non-radioactive filter hybridization. A plasmid containing *Xhip* was rescued and confirmed by sequencing. The missing 5′-end was amplified by RACE-PCR, RaceR-CTATACAATGTAGCTGGTCAGATCCAGCAAGATG (Clontech, USA). In total, a 2375 bp *Xhip* cDNA was isolated containing the open reading frame of 2091 bp. For RT-PCR primers were as follows: Xhip: F1-GAGGGGTGCAGGGGTCTTTATC, R1-TATCTGGCCTCGGCATGTGTAGTA; 5′UTR-Shh: F2-CTCATTTGCCCATAATTACTG, R2-CTCGTCCGAGCGAAGCCAATTA; siamois: F3-AAACCACTGATTCAGGCAGAGG; R3-GTAGGGCTGTGTATTTGAAGGG; Xnr3: F4-ATGGCATTTCTGAACCTGTTCTTC; R4-AGGTGGAACGGTGCTCACATGGAT.

Animals, microinjection procedures, and treatment

Production and rearing of embryos was as described (Hollemann et al., 1998). Staging of the embryos was done according to (Nieuwkoop and Faber, 1967). The coding region of murine *Hip1* and *Xenopus Hip* were subcloned into pCS2+ and constructs were checked by sequencing and in vitro translation (TNT kit, Promega). To generate mRNA for microinjection, plasmids were linearized and transcribed with SP6 as follows: *activin*: *Xba*I; *BMP4*: *Bam*HI; *Cerberus*: *Not*I; *Elk*: *Asp*718; *eFgf*: *Acc*I; *Fgf*: *Not*I; *LacZ*: *Not*I; *Xhip*, *mHip1*: *Not*I; *Noggin*: *Not*I; *Ptc*Δ*loop2*: *Not*I; *Xshh*: *Bam*HI, T7; *Xwnt8-myc*: *Asp*718; *Xwnt-3a*: *Eco*RI; *dnWnt-8*: *Asp*718; *XFD*: *Eco*RI (SP6 in vitro transcription kit, Ambion) or for *Chordin*: *Sfi*I, T3 (Stratagene, USA). RNAs were injected in 5 nl at concentrations of up to 400 pg/nl either alone or together with 10 pg/nl of *LacZ* RNA as lineage tracer. To compensate for mRNA concentration differences in co-injections, *LacZ* mRNA was added in equal quantities. Animal caps were excised at NF stage 8 (Gastromaster, XENOTEK, USA); sets of 10–15 caps were cultured for 4–24 h at RT in 0.5 ×MBS incl. Penicillin/Streptomycin. Cyclopamine treatment was performed at 200 μM after removing the vitelline membrane at stage 9. Morpholino oligonucleotides (MO), directed against a sequence in the 5′-UTR including the start-ATG of *Xhip* (5′-TGCTGCAAAACACCGTCCCACAAAG-3′) and standard control MO were purchased from Gene Tools LLC, resuspended in sterile, filtered water and 2.5 pmol/blastomere was injected into one cell of a two-cell stage embryo. For the rescue experiments, either 50 or 100 pg of capped *mHip1* RNA was co-injected with the Xhip morpholino.

Whole-mount in situ hybridization

RNA probes were made from plasmids digested and transcribed as follows: *Xbra*: *Bgl*II, T7; *CryA*: *Nco*I, Sp6; *Dlx3*: *Eco*RI, T7; *Emx2*: *Eco*RI, Sp6; *En-2*: *Xba*I, T3; *Fgf-8*: *Xba*I, T3; *Gsh-1*: Apa1, Sp6; *Xhip*: *Nco*I, Sp6; *Krox-20*: *Eco*RI, T7; *Xnkx-2.1*: *Not*I, T7; *Xotx2*: *Not*I, T7; *Xpax2*: *Eco*RI, T3; *Xpax6*: *Pst*I, T7; *Xpitx1*: *Nco*I, Sp6; *Xpitx3*: *Eco*RI, T7; *Xptc1*: *Bam*HI, T3; *Rhodopsin*: *Not*I, T7; *Rx*: *Xho*I, Sp6; *Xshh*: *Xba*I, T3; *Xsix3*: *Not*I, T7; *Xsox3*: *Eco*RI, T7; *Xvax1*: *Eco*RI, Sp6; *Xwnt-8*: *Bam*HI, T3. Double in situ hybridizations were done with digoxigenin and fluorescein-labeled RNAs followed by FastRed and NBT/BCIP staining, respectively. X-gal staining was performed prior to whole-mount in situ hybridization. Gelatine/albumin-embedded embryos were sectioned using a vibratome (Pelco, USA) as previously described (Hollemann et al., 1999).

Whole-mount immunostaining

For the detection of phosphorylated MAPK, embryos were incubated in 1× TBS, 5% BSA and 0.1% Triton-X-100 containing Phospho-p44/p42 MAP Kinase Antibody (Cell Signaling Technology) 1:400 over night in the cold-room. Anti-rabbit AP (Sigma) 1:1000 was used as secondary antibody for 5 h at room temperature, staining was performed using NBT/BCIP (Curran and Grainger, 2000).

Apoptosis/proliferation assay

For the detection of apoptotic cells (Hensey and Gautier, 1998), embryos were incubated in 0.5 μM Dig-11dUTP (Roche) and 150 U/ml TdT (Gibco BRL). Labeled DNA was visualized using anti-Dig-AP antibodies and NBT/BCIP. For BrdU labeling, embryos were injected with undiluted BrdU labeling reagent (Boehringer Mannheim) in the yolk at stage 10 or in the anterior gut of tailbud stage embryos (Eagleson et al., 1995). Following injection, embryos were transferred to 0.1× BS for 3 h, fixed 2 h in 4% PFA, incubated 1 h in 2 N HCl, rinsed with 1× PBS prior to BrdU immunodetection and plastic sectioned (5 μm). For hydroxyurea/aphidicolin (HUA) experiments devitellinized stage 10.5 embryos were incubated in 20 mM HU and 150 μM aphidicolin (Sigma) in 0.1× MBS (Harris and Hartenstein, 1991).

Results

Isolation and structure of the Hedgehog-interacting protein (Xhip) of Xenopus

To understand the function of *Hip* in early *Xenopus* development, we cloned the *hedgehog-interacting protein*

(*Xhip*) from *Xenopus* (GenBank accession no. AY328923). The predicted protein sequence is highly homologous to previously published *Hip* variants. Overall amino acid identities are 76% and 75% in a comparison of *Xhip* with human *Hip* and mouse *Hip1*, respectively (Fig. 1). As described for the mammalian *Hip* proteins, the predicted *Xenopus* HIP harbors an N-terminal signal peptide and a hydrophobic domain at the C-terminus, which is necessary

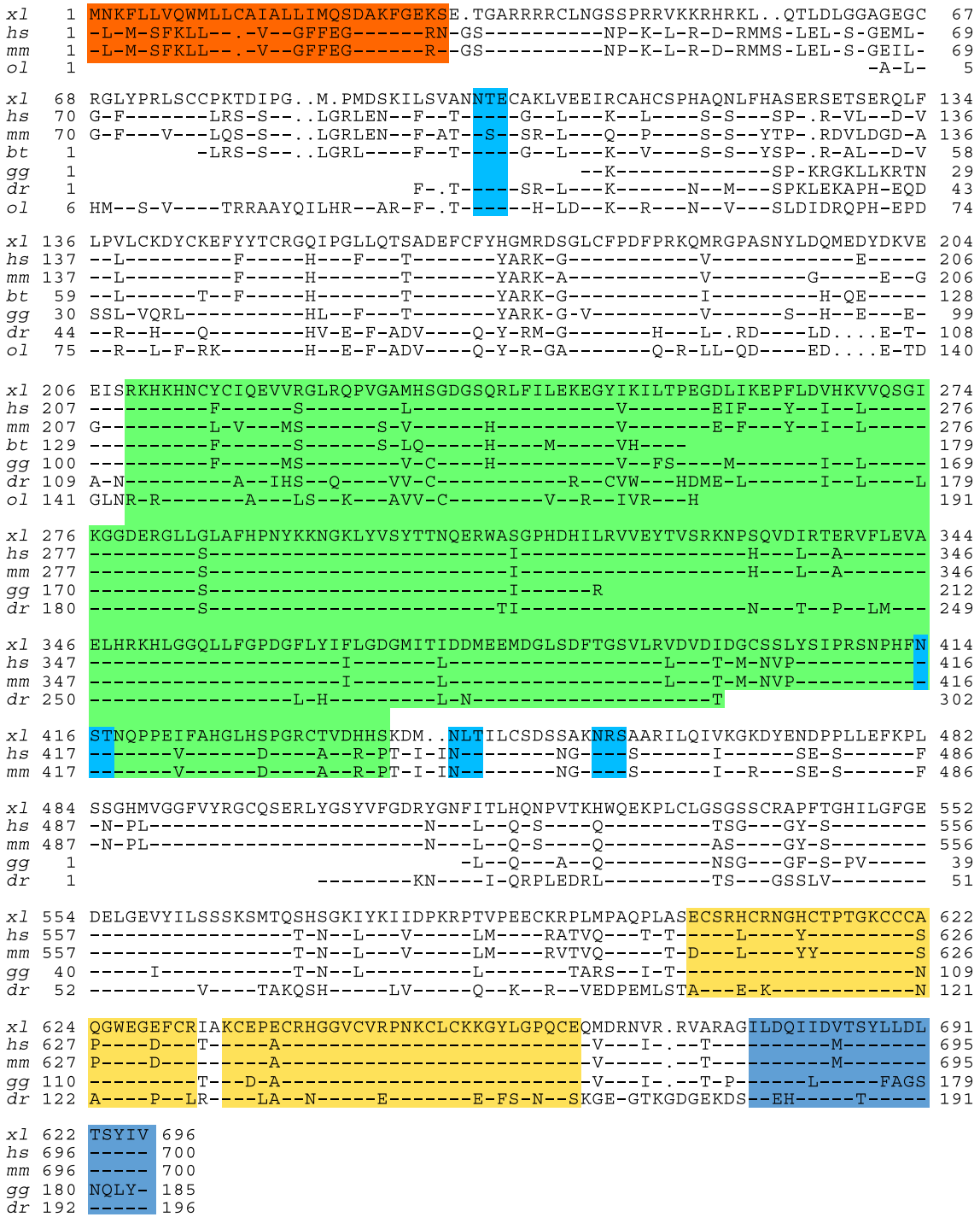

Fig. 1. Structure and amino acid alignment of *Xhip*. Sequence comparison of *Xenopus*, human (Ingham and McMahon, 2001) and mouse (Chuang and McMahon, 1999) HIP proteins. In addition, corresponding EST clones from medaka (G-Acc: AU170600), cattle (Gb-Acc: CB433643), chicken (Gb-Acc: BU132134, BU214137) and zebrafish (Gb-Acc: AW344287, AI878265, AW165324) are included. Identities are represented by hyphens. Gaps are reflected by dots. The putative signaling domain is shown in red. Four potential glycosylation sites are highlighted in blue. The predicted six 4-stranded beta-sheet motif is shown in green. Two EGF-like domains are represented in yellow and the hydrophobic membrane-anchoring domain at the C-terminus in light blue. Abbreviations: bt, *Bos taurus*; dr, *Danio rerio*; gg, *Gallus gallus*; hs, *Homo sapiens*; mm, *Mus musculus*; ol, *Oryzias latipes*; xl, *Xenopus laevis*; Gb-Acc: Genbank accession number.

to anchor the mature protein to the cell membrane, four potential glycosylation sites and two EGF-like modules (Chuang and McMahon, 1999). A computer-aided search (SMART at www.embl.de) for additional structural motifs within the HIP protein revealed the existence of a "six 4-stranded beta-sheet motif". This motif has first been described in soluble quinoprotein glucose dehydrogenase, but has been recently identified also in members of the low-density lipoprotein (LDL) receptor superfamily, such as Megalin and LRP6, and in the Wnt-inhibitory protein (WIF). WIF and LRP6 have been shown to interact with Wnt molecules, whereas Megalin binds to the N-terminal fragment of Sonic Hedgehog with high affinity (Hsieh et al., 1999; Jeon et al., 2001; McCarthy et al., 2002; Oubrie et al., 1999; Tamai et al., 2000). The domains listed above are highly conserved in HIP proteins previously identified in human, mouse, cow, chicken, zebrafish, and medaka. Recently, a partial cDNA was submitted that matches with *Xhip* but misses the 3′ end of the open reading frame (GenBank accession no. BC046952). However, no other closely related genes have been identified in *Xenopus* so far, and remarkably, no HIP protein or EST has been identified in non-vertebrates.

Temporal and spatial expression of Xenopus Hip

The first spatially restricted expression of *Xhip* is observed in two lateral domains adjacent to the anterior neural plate during neurulation (NF stage 18; Fig. 2a), corresponding to the presumptive placodal ectoderm including the lens anlage (Zygar et al., 1998). As neurulation proceeds (NF stage, 20; Figs. 2b, c, c′), *Xhip* expression is detected in the region of the future lateral line placodes, which is found to become separated into the anterodorsal, anteroventral, middle and posterior lateral line placodes, the facial, glossopharyngeal, 1st, 2nd, 3rd vagal epibranchial placode, and in migrating neural crest cells of the branchial arches in early tailbud stage embryos (NF stage 24; Fig 2d, e) and tadpole embryos at NF stage 34 (Figs. 2g, h; Schlosser and Northcutt, 2000). Furthermore, dispersed *Xhip*-positive cells are found more posterior to the head region in the lateral mesoderm at NF stage 20 (Figs. 2b, c). Within the closing neural plate, low-level expression of *Xhip* is observed in two paraxial stripes at stage 18, which later mark two clusters of cells within the ventral part of the neural tube, presumably oligodendrocyte precursors at NF stage 28 (Fig. 2f; Zhou et al., 2000). In addition, high levels of *Xhip* transcripts are detected within the placodes of the olfactory system, the pineal gland and in the mesenchyme of the branchial arches (Figs. 2g, h). Interestingly, transient expression of *Xhip* is observed in the chorda dorsalis at NF stages 20 and 24 that disappears by NF stage 28 (Figs. 2c′, e′, f). In NF stage 41 tadpoles, *Xhip* expression is observed in a thin rim at the edge of the mouth opening and at the transition zone of the yolk mass toward the forming anus (Fig. 2i). In addition, *Xhip*-positive cells are found in the lower jaw (Figs. 2j, k). Taken together, *Xhip* expression is found mainly in neurogenic placodes and neural crest derived structures, but also close to or in Shh-positive areas (see also Figs. 4D, a–b″; Ekker et al., 1995).

Regulation of Xhip expression in whole embryos and in neuralized animal cap explants

Overexpression studies in mice have indicated that Shh is able to induce *mHip1* expression within the developing endochondral skeleton (Chuang and McMahon, 1999). Therefore, we tested if Shh can also induce *Xhip* expression in *Xenopus* embryos (Figs. 3a–c). Injection of *Shh* mRNA caused a significant activation of the *Xhip* gene, but only in cells that normally express *Xhip*, or in cells that are located directly adjacent to the regular expression domains (58%, $n = 26$). Thus, the competence for *Hip* gene activation by Shh is spatially restricted.

Since not all Hip expression domains were found to be close to Hh expressing cells, we next examined the regulation of *Xhip* expression in animal cap explants by secreted proteins that had been shown to influence early neural patterning (Fig. 3d). Microinjected mRNA encoding either *BMP4*, *eFgf*, *Shh*, *Wnt-8*, *Chordin*, and *Cerberus* failed to activate *Xhip* expression significantly. In contrast, mRNA injection of the dorsalizing TGFβ-type signaling molecule activin strongly induced *Xhip* and *Shh* expression. In addition, we tested induction of *Xhip* in animal caps neuralized by the BMP-antagonist Chordin. *Xhip* expression was observed in explants injected with *Chordin* in combination with either *Shh* or *Wnt-8*, but not with *eFgf*. Co-injection of *Chordin* and *Shh* together with *Wnt-8* did not result in an enhanced activation of *Xhip* above levels of expression seen with *Chordin* and *Shh* alone. Furthermore, we noticed that the induction of *Xhip* coincides with the autoinduction of *Shh* in neuralized explants; induction of *Shh*, but not of *Xhip*, was enhanced by additional *eFgf*. Interestingly, the induction of *Xhip* by *Wnt-8* was not Shh-dependent. Moreover, co-injection of *Wnt-8* along with *Chordin* and *Shh* even inhibited the autoinduction of *Shh*. Taken together, activin was the only signaling molecule found to be sufficient to induce *Xhip* in animal caps, whereas *Shh* and *Wnt-8* could promote *Xhip* expression only in neuralized explants.

Hip is a multifunctional antagonist of Hh, Fgf, and Wnt-8 pathways

Previous studies had indicated that the Hip1 protein binds specifically to all Hedgehog N-terminal fragments thereby inhibiting Hh signaling (Chuang and McMahon, 1999). However, it was not reported if Hip1 interferes with the activity of other secreted signaling molecules as well. First, we examined if Hh signals can be inhibited by mHip1 in animal cap explants. We could not detect the induction of either *Shh* or the Hh target gene *Ptc1* in

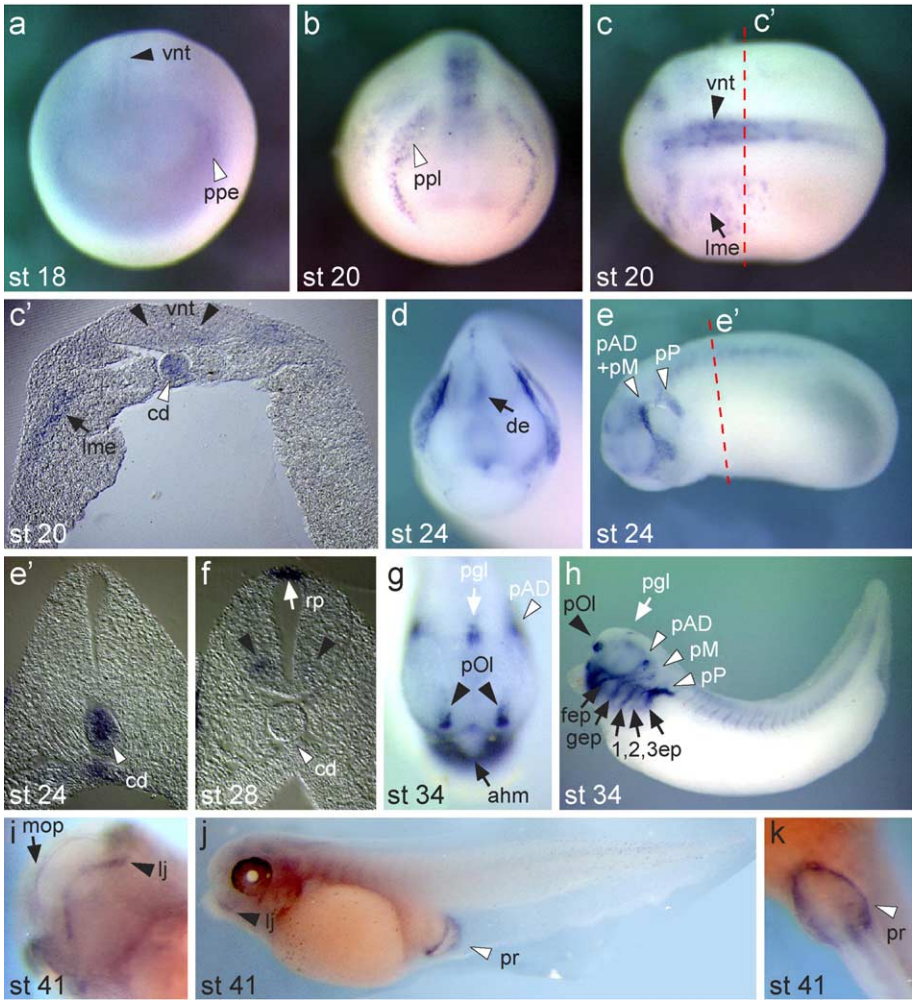

Fig. 2. Temporal and spatial expression of *Xhip*. Whole mount in situ hybridization of *Xhip* in *Xenopus* embryos. Staging according to Nieuwkoop and Faber (1967). (a) Neurula stage (NF stage 18), anterior view. White arrowhead, preplacodal ectoderm; black arrowhead, expression of *Xhip* in paraxial stripes in the ventral neural tube. (b) Early tailbud (NF stage 20), frontal view. Arrowhead, presumptive placodal epithelium. (c) Dorsal view, anterior to the left. Arrow, lateral mesoderm; arrowhead, ventral neural tube. (c′) Transversal section. White arrowhead, chorda dorsalis; arrow, lateral mesoderm; black arrowheads, paraxial stripes in the ventral neural tube. (d) Mid-tailbud (NF stage 24), frontal view. Arrow, diencephalon. (e) Lateral view, anterior to the left. White arrowhead, pAD + pM, common anterodorsal and middle lateral line placode; white arrowhead, pP, posterior lateral line placode. (c′, e′, f) Transversal sections reveal *Xhip* expression in the chorda dorsalis at NF stages 18 and 24, but not at NF stage 28 (white arrowheads). (f) Expression of *Xhip* in the roof plate (white arrow), *Xhip* dorsal to the floor plate (black arrowhead). (g) In tailtip stage embryos (NF stage 34), frontal view, *Xhip* is expressed in the pineal gland (white arrow), in the anterodorsal lateral line placode (white arrowhead), in the olfactory placodes (black arrowhead) and in the anterior head mesenchyme (black arrow). (h) Lateral view, anterior to the left. A black arrowhead indicates *Xhip* expression in the olfactory placode. White arrow, pineal gland anlage. White arrowheads, anterodorsal, middle and posterior lateral line placode; black arrows from anterior to posterior, facial epibranchial placode fused with the anteroventral lateral line placode, glossopharyngeal placode, 1st, 2nd, and 3rd vagal epibranchial placode. (i) Ventral view of the head of the tadpole shown in j (NF stage 41); arrowhead, lower jaw; arrow, rim of the mouth opening. (j) Lateral view, anterior to the left. Black arrowhead, lower jaw; white arrowhead, rim-like staining for *Xhip* at the transition zone between the yolk mass and the ectoderm. (k) Ventral view of the proctodeum of the tadpole shown in j, white arrowhead as in j. Abbreviations: 1,2,3ep, 1st, 2nd, and 3rd vagal epibranchial placode; ahm, anterior head mesenchyme; cd, chorda dorsalis; de, diencephalon; fep, facial epibranchial placode fused with the anteroventral lateral line placode; gep, glossopharyngeal placode; mop, mouth opening; lj, lower jaw; lme, lateral mesoderm; pAD, anterodorsal lateral line placode; pgl, pineal gland; pM, middle lateral line placode; pOl, olfactory placode; pP, posterior lateral line placode; ppe, preplacodal ectoderm; ppl, presumptive placodal epithelium; pr, proctodeum; rp, roof plate; vnt, ventral neural tube.

control caps, or in explants neuralized with *Chordin* or injected with Shh alone, respectively (Figs. 4A, a–c and data not shown). However, *Ptc1* expression was strongly induced by the co-injection of *Chordin* and *Shh* as reported before (Tsuda et al., 2002), whereas the addition of *mHip1* inhibited the induction of *Ptc1* by *Shh* in neuralized explants (Figs. 4A, d, e). Although *Chordin* and *Shh* can induce *Xhip* expression (Fig. 3d), the level of induction was apparently not sufficient to inhibit an excess of Shh molecules. To further test if Hip inhibits only Shh or interferes with other secreted signaling molecules, we injected mRNA for *mHip1* together with *BMP4*, *activin*, *eFgf*, and *Fgf-8*. All of these peptide growth factors can induce *Xbra* expression in animal cap explants (Christen and Slack, 1997; Northrop et al., 1995; Schulte-Merker and Smith, 1995). In early explants (NF stage 10.5) neither

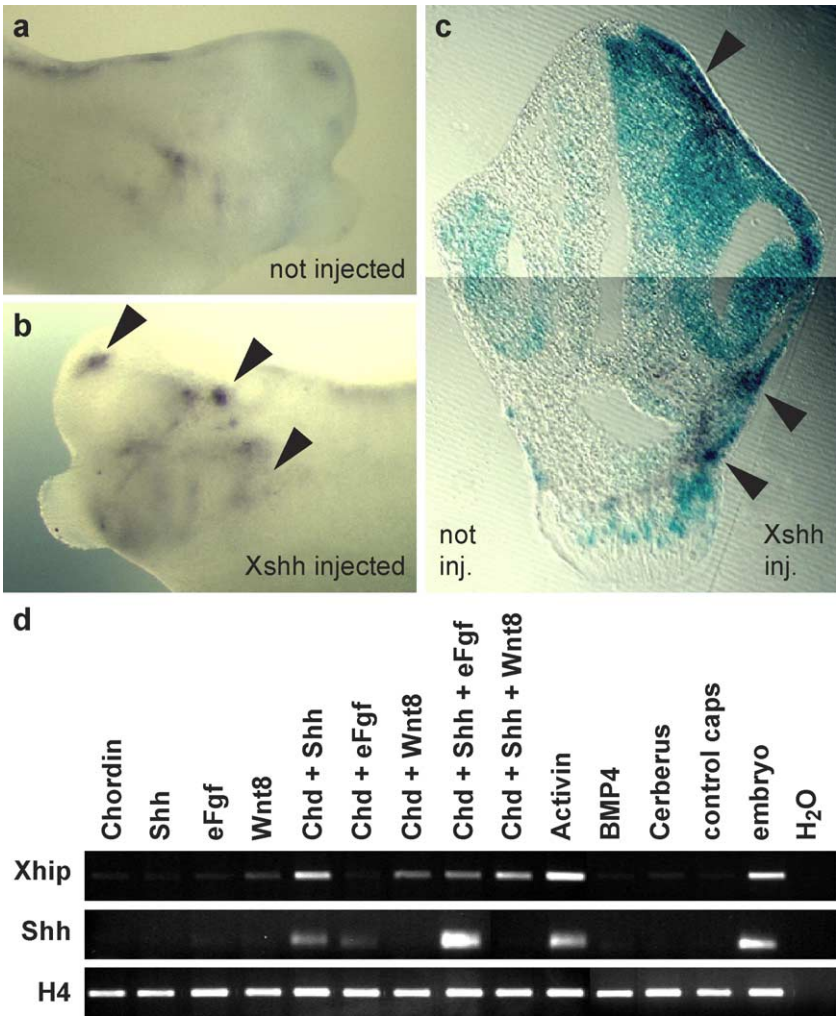

Fig. 3. Regulation of *Xhip* expression in whole embryos and animal caps explants. Enhanced *Xhip* expression (b, c, arrowheads) induced by *Xshh* mRNA injection (500 pg) in embryos at NF stage 34. (a) Uninjected, and (b) injected side of the same embryo. (c) Transversal section of an embryo co-injected with *LacZ* mRNA (light blue). (d) Two-cell stage embryos were injected with mRNA of *Chordin* (*Chd*, 50 pg), *Shh* (500 pg), *eFgf* (10 pg), *Wnt-8* (50 pg), *activin* (1 pg), *BMP4* (1 ng), *Noggin* (50 pg) or *Cerberus* (200 pg). RT-PCR analysis of animal cap ectoderm was done corresponding to NF stage 19. Expression of *Xhip* was induced by a combination of *Chordin* and *Shh* or *Wnt-8*, as well as by *activin*.

BMP4 nor *activin* was inhibited by co-injection with *mHip1* mRNA (Figs. 4A, g–j), although we observed a suppression of *Xbra* induction by *mHip1* in late explants (NF stage 17) (Figs. 4A, l–o). In contrast, we observed a strong inhibition of *Fgf* activity as monitored by the suppression of *Xbra* induction, when either *eFgf* or *Fgf-8* was co-injected with *mHip1* (Figs. 4A, q–v). The inhibition of *Xbra* expression was partially released by the co-injection of *Elk* (Fig. 4A, w), which is an intracellular mediator of the Fgf signal (Janknecht et al., 1993). Since *Elk* could rescue the inhibition of *Fgf* signaling by secreted Hip, the inhibition of *Fgf* signaling occurred most likely at or upstream of the corresponding FGF receptor.

To further investigate the influence of *Hip* on eFGF-dependent MAPK phosphorylation and on *Xbra* gene activation in whole embryos, we analyzed *mHip1*-injected embryos at early gastrula stage. At NF stage 10, transcripts of *Xbra* and phosphorylated MAPK protein can be detected in a complete ring around the blastopore (Figs. 4B, a, c; (Curran and Grainger, 2000). The injection of *mHip1* mRNA resulted in suppression of *Xbra* expression (72%, $n = 25$) and of MAPK phosphorylation (67%, $n = 15$), as monitored by whole-mount in situ hybridization for *Xbra* and immunostaining for MAPK-P, respectively (Figs. 4B, b–b′, d–d′).

Since Wnt signals induce *Xhip* expression in neuralized explants, we examined if *Hip* exerts an influence on the Wnt pathway, using the double axis formation assay (Wang et al., 1997b). *Wnt-3a* and *Wnt-8* mRNA injection led to the formation of a secondary axis in approximately 80% of the embryos (Figs. 4C, a, b, e). While the co-injection of *mHip1* and *Wnt*-3a neither suppressed nor enhanced the *Wnt-3a* induced formation of a secondary axis, we observed a strong suppression when *mHip1* was co-injected with *Wnt-8*, indicating that *Hip* can interfere specifically with the *Wnt-*

8 pathway (Figs. 4C, c, d, e). Injection of *Wnt-8* and *Wnt-3a* was demonstrated to induce expression of *Xnr3* and *siamois* (Bell et al., 2003). RT-PCR analysis of animal cap explants revealed *Hip*-mediated suppression of *Xnr3* and *siamois* induction by *Wnt-8*, but not by *Wnt-3a* (Fig. 4C, f). Taken together, these results indicate that while *Hip* is a non-selective inhibitor of Hh and Fgf signaling, it specifically interferes with the Wnt-8 but does not interfere with the Wnt-3a pathway.

Xhip is expressed in regions close to Shh-, Wnt-8-, and Fgf-8-positive cells

Since Hip was found to interact with Shh, Wnt-8, and Fgf-8, we wanted to investigate if they are expressed in adjacent or overlapping regions during development. At tadpole stage, *Shh* is expressed in the inner neural layer of the ventral diencephalon up to the prospective sulcus limitans, as well as in the floor plate, whereas *Xhip*-expressing cells were found within the sulcus limitans, and in the ventricular layer dorsally to the *Shh* domain, respectively (Figs. 4D, a′, b′, a″, b″). Thus, *Shh* and *Xhip* are expressed in adjacent, non-overlapping territories. *Xenopus Hip* is also localized in many areas that are not close to sites of *Shh* expression, such as the olfactory placodes and the placodes of the cranial nerves. Therefore, the reported expression pattern for *Bhh* and *Chh* suggests a possible interaction of *Xhip* and *Bhh* or *Chh* during early development as well (Ekker et al., 1995). However, a careful reinvestigation of *Bhh* and *Chh* expression revealed that both are not expressed as reported previously and therefore are not supposed to interact with *Xhip* in early stages (Supplementary Fig. 3). We also included expression analysis of *Fgf-8* that is expressed in prospective forebrain regions (Christen and Slack, 1997), as well as of *Xwnt-8*, which we found to be inhibited by *mHip1*. Most strikingly, in horizontal sections at the level of the foregut, we found the expression of *Xhip*, *Shh* and *Fgf-8* to be almost mutually exclusive. *Shh*-positive cells were found in the foregut endoderm and in the posterior endothelium of the visceral pouches, whereas *Fgf-8* expression was detected more anteriorly. *Xhip* was expressed in close proximity within the adjacent mesenchyme of the branchial arches (Figs. 4D, a‴, b‴, c′). During neurulation, we found expression of *Xhip* in the preplacodal region, adjacent to *Fgf-8*. More rostrally, the *Fgf-8*-positive cells are part of the anterior neural ridge (ANR); caudally, they form a thin band surrounding the ventral half of the embryo, which may demarcate the transition zone between the placodal area and the ventrolateral non-neural ectoderm (Figs. 4D, d–f). Interestingly, *Xwnt-8*-expressing cells were detected at the caudal limits of both *Fgf-8*-positive stripes within the prospective head region (Fig. 4D, g). To summarize, *Xhip*-positive cells appear in domains that are close to territories of *Shh*, *Xwnt-8*, and *Fgf-8* expression.

Modulation of visual system and olfactory development

Previously, we have reported that the overexpression of *mHip1* resulted in the induction of ectopic otic vesicles in *Xenopus* embryos and in a strong upregulation of the preplacodal marker *Eya1* and of *Pax8*, an early marker for otic ectoderm (Koebernick et al., 2003). To extend these studies, we concentrated on how the overexpression of *Hip* influences the development of structures that are derived from the anterior neural plate and preplacodal domain. Although we made use of the murine *Hip1* in all our overexpression studies, the microinjection of *Xenopus Hip* resulted in the development of identical phenotypes. Most strikingly, unilateral injection of *mHip1* or *Xhip* mRNA injection caused an enormous enlargement of the eye in embryos at NF stage 33/34 (Fig. 5A, a and Supplementary Fig. 1). Sectioning of *mHip1* or *Xhip* mRNA-injected embryos revealed that almost all cells of the midbrain and of the caudal part of the forebrain had adopted a retinal fate, as monitored by *Xrx1* expression (Fig. 5A, a′, Supplementary Fig. 1), whereas the optic stalk marker *Vax1* was repressed (Figs. 5A, b–b′). In contrast, when *Shh* mRNA was injected, it caused the induction of the optic stalk marker *Vax1* in the remaining optic vesicle at the expense of retinal markers, such as *Pax6* and *Xrx1* (Figs. 5A, h–i′; (Hallonet et al., 1999; Macdonald et al., 1995). The giant eye-like structures induced by *mHip1* still preserved some stratification, although misplaced patches of photoreceptor cells were detected, as visualized by *rhodopsin* expression (Figs. 5A, c–c′), whereas Shh did suppress *rhodopsin* expression (Figs. 5A, j–j′). Interestingly, examination of the lens and olfactory placode revealed that the lens and olfactory territory was also enlarged upon *mHip1 injection*, which was examined by *Crystallinα* and *Emx2* expression (Figs. 5A, d–e′). However, lens formation was abnormal since lens invagination did not occur, and as a result, the remaining lens tissue was arrested in a placodal-like state (Fig. 5A, d′). In contrast, a complete repression of lens and olfactory placode induction was observed in *Shh*-injected embryos (Figs. 5A, k–l′). In addition, we examined the dorsoventral patterning of anterior CNS, which depends on the formation of an Hh gradient, emanating from the chorda dorsalis and floorplate (Ericson et al., 1995). In *mHip1*-injected embryos, the amount of transcripts for *Nkx-2.1* in the ventral forebrain appeared to be reduced (Figs. 5A, f–f′), whereas the expression of the homeobox-containing gene *Gsh-1*, a marker for the territory of intermediate neurons (cloning and detailed description of *Xenopus Gsh-1* will be published elsewhere), was expanded ventrally (Figs. 5A, g–g′), as opposed to *Shh*-injected embryos (Figs. 5A, m–n′). Taken together, the microinjection of *Shh* induced eye stalk fate at the expense of retina and lens development, whereas *Hip* overexpression enlarge retinal structures at the expense of presumptive brain region.

Since *Xhip* is expressed in the olfactory and lens placodes during development and also interfered with Fgf-

A
ptc1
Xbra
st 17
st 10.5
st 17
st 10.5
st 17
not inj.
Chordin
Shh
Chordin +Shh
Chordin +Shh+Hip
not inj.
BMP4
BMP4 +Hip
Activin
Activin +Hip
Hip
BMP4
BMP4 +Hip
Activin
Activin +Hip
Hip
eFGF
eFGF+Hip
eFGF
eFGF+Hip
FGF8
FGF8 +Hip
eFGF+Hip +Elk
B
Xbra
MAPK-P
-Hip
+Hip
C
+ Wnt3a
+ Wnt8
-Hip
+Hip
1°
2°
D
Shh
Hip
Fgf8
Shh
Hip
Shh
Hip
Fgf8
Shh
Hip
Fgf8
Wnt8
e
secondary axis (%)
84 %
71 %
78 %
10 %
Wnt3a
Wnt3a +Hip
Wnt8
Wnt8 +Hip
f
Xwnt3A
Xwnt3A + Hip
Xwnt8
Xwnt8 + Hip
control caps
embryo
H2O
Xnr3
siamois
H4

8 and Wnt-8 pathways, we investigated the impact of these signals on olfactory and lens induction further. Expression of a dominant-negative form of *Xwnt-8* (dnXwnt-8) led to the formation of embryos with enlarged anterior structures (Hoppler et al., 1996). The enlarged heads also included enlarged olfactory and lens placodes, as we demonstrated by the expression of *Emx2* and *Pitx3* in embryos at NF stage 34 (Figs. 5B, a–b″). Although the arrangement of other structures of the embryonic head, such as the telencephalon, the midbrain–hindbrain boundary and the rhombomeres 3/5 were almost normal, the expression level of the respective marker genes was enhanced (Figs. 5B, a–a″). In *Xenopus*, Fgf signals contribute to the formation of posterior neural tissue (Ribisi et al., 2000). Although the microinjection of a dominant-negative form of the Fgf receptor 1 (XFD) did not alter the size of the olfactory placode, we observed a minor increase of the lens territory (Figs. 5B, c–d″). In contrast, microinjection of a small dose of *Fgf-8* mRNA (10 pg) was sufficient to completely suppress the induction of the olfactory and lens placode and eye development. However, with this dose of *Fgf-8* mRNA injected, the expression of *Emx2* in the telencephalon was not altered and the expression of *En-2* in the midbrain–hindbrain boundary was even strengthened (Figs. 5B, e–f″ and Supplementary Fig. 2b). Thus, while the activation of Shh, Wnt-8, and Fgf signaling led to a suppression of placode formation, the individual inhibition of either Wnt-8 or Fgf signaling resulted in larger lens and, as shown for dnWnt-8, in larger olfactory placodes. In line with these results, the simultaneous inhibition of the pathways mentioned led to an enlargement of these placodes by *Hip* alone.

Hip overexpression increases the number of retinal and lens precursors

To understand the relative timing of the enlargement of anterior neural structures, we investigated the effect of *Shh* and *mHip1* mRNA-injections on the induction of the visual system primordium at NF stage 14, when retinal precursors are born (Fig. 6A). *mHip1* overexpression led to a strong increase in the number of *Rx1*-positive cells extending the original domain, while additional Hh resulted in a reduction of *Rx1* expression (Figs. 6A, a, g). We never observed ectopic *Rx1* expression distinct from the primary domain, indicating a dependence of *Rx1* expression on anterior competence. Accordingly, we found that overexpression of *mHip1* mRNA strongly expanded the expression domains of *Pax6*, *Six3*, and *Otx2*, all known to be indispensable for eye development (Figs. 6A, b–d), while microinjection of Shh did not change the expression of *Pax6*, *Six3*, and *Otx2* (Figs. 6A, h–j). In addition, we noticed that *Pitx1*, a marker for lens preplacodal ectoderm, was up-regulated upon *mHip1* injection. Most interestingly, ectopic *Pitx1* expression still maintained the spatial organization in respect to *Pax6* (Fig. 6A, b), with which it marked the anterior border of the neural plate and lateral the presumptive lens ectoderm (Hollemann and Pieler, 1999). These results suggest that the expansion of the anterior neural plate was at the expense of non-neural ectoderm. However, the lateral neural plate was still under the influence of signals emanating from the remaining non-neural ectoderm. Indeed, *Dlx3* expression, which depends on an intermediate level of BMP and demarcates the border between the non-neural and neural ectoderm (Woda et al., 2003), was shifted laterally (Figs. 6A, e–f). However, the microinjection of *Shh* mRNA did not alter the pattern of *Dlx3*, although the level of *Dlx3* expression was slightly increased (Figs. 6A, k–l). Since the microinjection of *Shh* mRNA did not change the formation of anterior neural plate significantly, we investigated if the inhibition of Wnt-8 or Fgf signaling contributed to the altered expression of *Six3* and *Dlx3* upon *mHip1* overexpression. While dnWnt-8 led to a strong induction of *Six3* and repression of *Dlx3* in early neurula stage embryos (Figs. 6B, a–b) (NF stage 13), overexpression of XFD did not

Fig. 4. *Hip* as multifunctional antagonist of Shh, eFgf/Fgf-8 and Wnt-8 signaling pathways. (A) *mHip1* inhibits Shh and eFgf pathways in animal cap explants. (a–e) Explants corresponding to NF stage 17. In situ hybridization with *Ptc1* as a marker for active Shh signaling. (a, b, c) Control caps and caps either injected with *Chordin* (50 pg) or *Shh* (500 pg) mRNA do not express *Ptc1*. (d) Co-injection of *Chordin* and *Shh* mRNA (500 pg) induces *Ptc1*. (e) *mHip1* mRNA (1 ng) suppresses *Ptc1* induced by *Chordin* and *Shh*. (f–w) Explants stained for *Xbra* at NF stage 10.5 or stage 17, respectively. (f) Control caps and caps injected with *mHip1* mRNA (k, p) do not express *Xbra*. (g, l) *Xbra* expression induced by *BMP4* mRNA (1 ng) or by *activin* mRNA (5 pg; i, n) is not blocked by *mHip1* in early explants (h, j) but in late explants (m, o). The induction of *Xbra* by either *eFgf* mRNA (10 pg; q, u) or *Fgf-8* (150 pg; s) is inhibited by the co-injection of *mHip1* (r, t, v), but *Xbra* expression is rescued by *Elk* mRNA (w, 300 pg). (B) (a–d′) Early gastrula stage embryos (NF stage 10), vegetal view. (a, b, b′) *Xbra* in situ hybridization and (c, d, d′) immunostaining of phosphorylated MAPK (MAPK-P). (a, c) Control embryos, *Xbra* and MAPK-P staining around the blastopore. Microinjection of *mHip1* mRNA (750 pg) into one cell of a four cell stage embryo inhibits expression of *Xbra* (b, b′; 72%, $n = 25$) and phosphorylation of MAPK (d, d′; 67%, $n = 15$). *LacZ* mRNA was co-injected as a lineage tracer (light blue). (C) (a, b, e) Second axis formation induced by *Wnt-3a* (a; 0.5 pg; 84% 2° axis; $n = 57$) or *Wnt-8* mRNA (b; 5 pg; 78% 2° axis, $n = 49$). Co-injection of *mHip1* (600 pg) did not block *Wnt-3a* (c; 71% 2° axis; $n = 32$), but *Wnt-8* activities (d; 10% 2° axis, $n = 39$). RT-PCR analysis of animal caps at NF stage 10.5. (f) Induction of *Xnr3* and *siamois* by *Wnt-8* (50 pg), but not by *Wnt-3a* (e; 0.5 pg), was inhibited by *mHip1*. (D) Comparison of *Xhip*, *Shh*, *Fgf-8*, and *Wnt-8* expression. (a, b, c) Lateral views, anterior to the left. (a′, a″, b′, b″) Transversal sections. *Shh* expression in the ventricular layer of the ventral diencephalon (arrow), while *Xhip* expression was detected near the sulcus limitans (arrow) in early tadpoles. (a″) *Shh* expression was found in the chorda dorsalis (red arrowhead) and floorplate (white arrowhead) and (b″) *Xhip* transcripts only dorsally to the floorplate (black arrowhead). (a‴, b‴, c′) Horizontal sections, anterior up. (a‴) *Shh* transcripts were detected in the posterior endothelium of the endodermal visceral pouches (black arrow) and *Fgf-8* in the anterior endothelium (c′, black arrow), whereas (b‴) *Xhip* expression was detected in the adjacent mesenchyme of the branchial arches (arrow). (d, e, f, g) Anterior view of neurula stage embryos. (d) Cleared embryo. *Shh* transcripts in the chorda dorsalis (white arrow) and prechordal plate (black arrow). (e, f) *Xhip* expression in the preplacodal region (white arrowhead) limited by *Fgf-8* transcripts in the anterior neural ridge (black arrowhead) and in a line outside the neural plate (red arrowhead). (g) *Xhip* in the lateral placodes is juxtaposed toward *Wnt-8* positive cells (arrow, arrowhead).

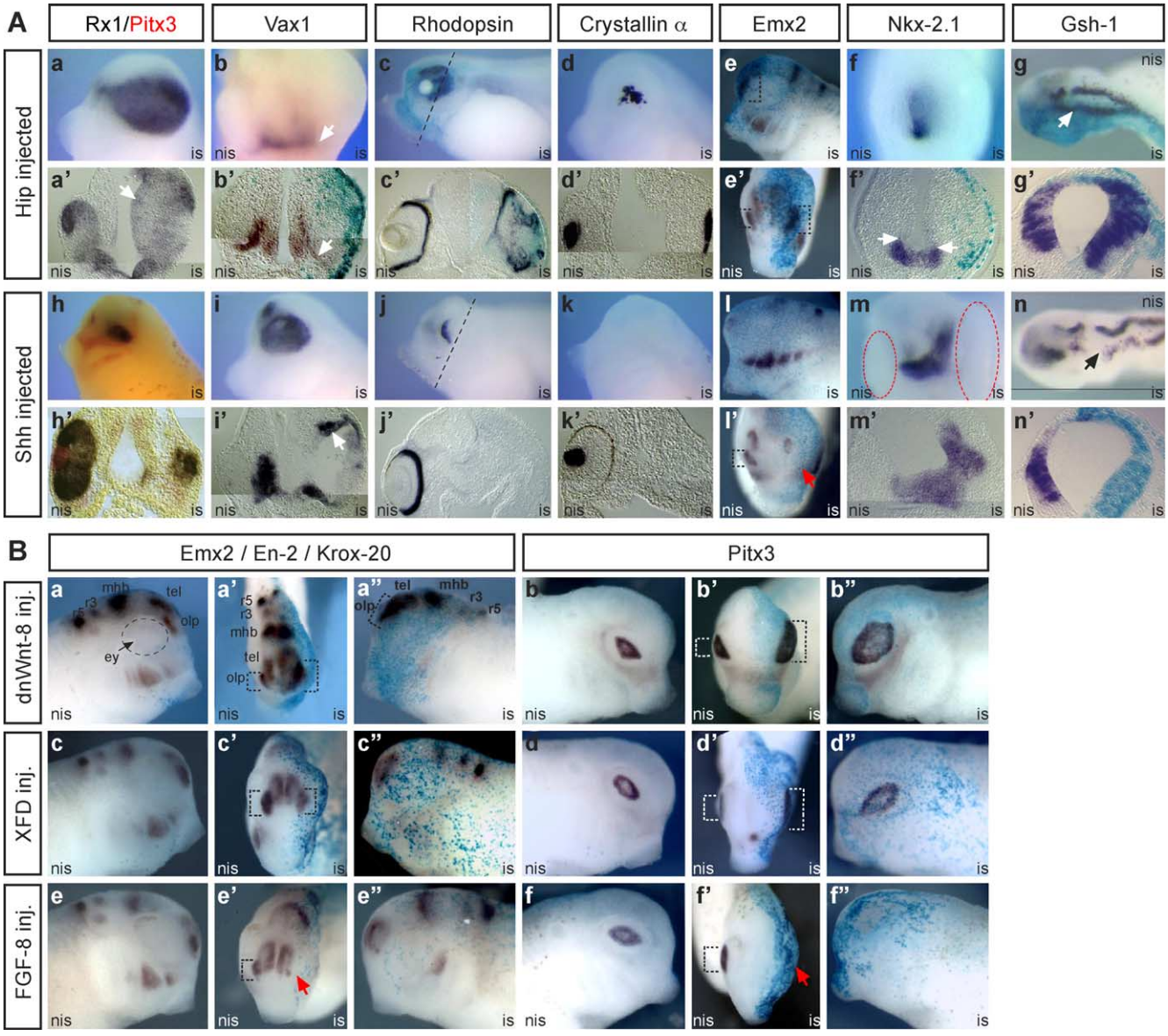

Fig. 5. The inhibition of Shh, Fgf and Wnt-8 signaling affects eye, brain, and placode development in tadpole stage embryos. (A) Overexpression of *mHip1* and *Shh*. (a–g′) Microinjection of *mHip1* (750 pg) into one cell of two-cell stage embryos. (h–n′) Overexpression of *Shh* (500 pg) into one cell of two-cell stage embryos. (b, e′, f, l′, m) Frontal view. (a, c, d, e, h, i, j, k, l) Lateral view. (g, n) Dorsal view. (a′–d′, f′, g′, h′–k′, m′, n′) Transversal sections. (a, a′) Formation of a giant eye. Note *Xrx1*-positive cells extend into the prospective midbrain region (white arrow in a′, 67%, $n = 18$). (b, b′) Repression of optic stalk marker *Vax1* within the ventral fore- and midbrain (white arrows, 63%, $n = 28$). (c, c′) Displaced *Rhodopsin* positive cells in the enlarged eye (76%, $n = 21$). (d, d′) Abnormal lens formation revealed by *Crystallin* α expression (50%, $n = 12$). (e, e′) Enlarged olfactory placode as revealed by *Emx2* expression, indicated by dashed open rectangles (65%, $n = 17$). (f, f′) Ventral shift of the dorsal limit of *Nkx-2.1* expression (white arrows in f′, 55%, $n = 11$). (g, g′) Ventral expansion of *Gsh-1* expression (38%, $n = 8$). (h–h′) Note the reduction of retinal tissue (*Xrx1,* dark brown) and lens tissue (*Pitx3,* red, 50%, $n = 10$). (i, i′) Expanded expression domain of the optic stalk marker *Vax1* (white arrow in i′, 62%, $n = 13$). (j, j′) Loss of *Rhodopsin* positive cells (83%, $n = 16$). (k, k′) Absence of lens specific *Crystallin* α expression (57%, $n = 14$). (l, l′) Suppression of olfactory placode development as revealed by the loss of *Emx2* expression, indicated by a red arrow (65%, $n = 17$). The dashed open rectangle marks the olfactory placode on the non-injected side (l′). (m, m′) Dorsal shift of ventral forebrain tissue as revealed by *Nkx-2.1* expression (56%, $n = 16$), the eye structures are emphasized by dashed ellipses. (n, n′) Reduced expression of the dorsal neural tube marker *Gsh-1* in the prospective midbrain (black arrow, 42%, $n = 12$). *LacZ* mRNA was co-injected as a lineage tracer (light blue in b′, c, c′, e, e′, f′, g, g′, l, l′, n′). (B) Influence of *dnWnt-8*, *XFD* and *Fgf-8* overexpression on lens and olfactory placode development. (a′, b′, c′, d′, e′, f′) Frontal views, dashed open rectangles indicate the size of the olfactory and lens placodes, respectively. (a, a″, b, b″, c, c″, d, d″, e, e″, f, f″) Lateral views. (a–b″) Overexpression of *dnWnt-8* (500 pg) resulted in enlarged olfactory (*Emx2*; 76%, $n = 22$) and lens placodes (*Pitx3*; 78%, $n = 18$). (c–d″) *XFD* (1 ng) injection did not alter the size of the olfactory placode but led to enlarged lens placodes (83%, $n = 16$). (e–f″) Additional *Fgf-8* (10 pg) inhibits olfactory and lens placode induction (red arrows in e′ and f′; 76%, $n = 19$). (a–a″, c–c″, e–e″) *Krox-20* and *En-2* expression was followed to control hindbrain and midbrain–hindbrain formation, respectively. *LacZ* mRNA was co-injected as a lineage tracer (light blue in a′, a″, b′, b″, c′, c″, d′, d″, e′, e″, f′, f″). Abbreviations: ey, eye cup; mhb, midbrain–hindbrain boundary; olp, olfactory placode; r3, rhombomere 3; r5, rhombomere 5; tel, telencephalon.

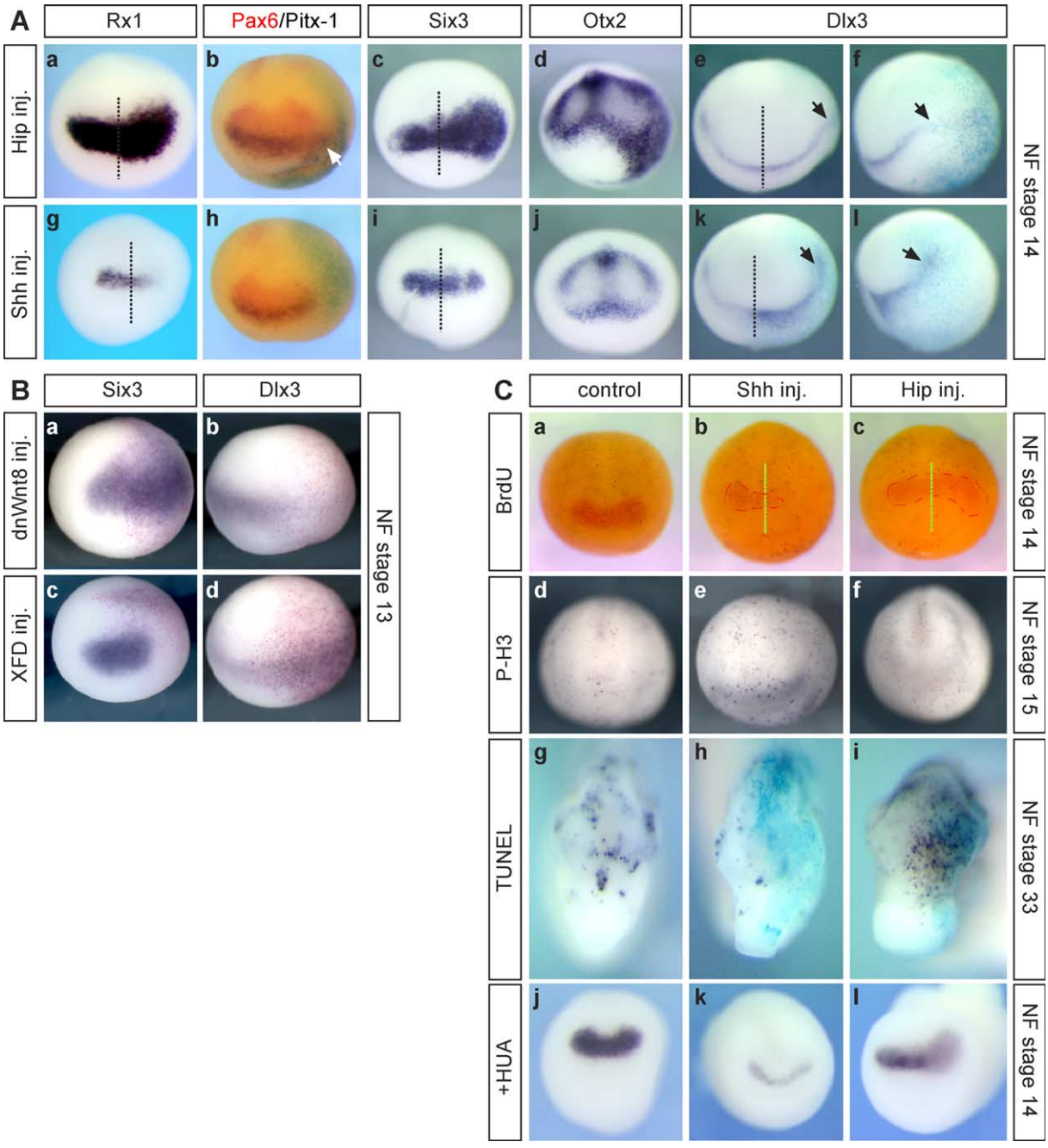

Fig. 6. Regulation of early eye field formation by *Hip* and *Shh.* (A) (a–e, g–k) Frontal views of embryos at NF stage 14, injected side to the right. (f, l) Lateral views of e and k. (a) Increased number of retinal progenitors upon *mHip1* overexpression (750 pg; 71%, $n = 46$). (g) Reduction of *Xrx1* expression after injection of *Shh* (500 pg; 50%, $n = 32$). (b, h) While *Shh* overexpression results in a slight reduction of *Pax6* expression in the anterior neural plate and *Pitx1* expression in the early lens field (45%, $n = 11$), both genes are up-regulated and expanded laterally after *mHip1* injection (67%, $n = 9$). Microinjection of *mHip1* mRNA results in strongly expanded domains of *Six3* and *Otx2* (c, 60%, $n = 10$; d, 100%, $n = 8$), but are almost normal upon *Shh* overexpression (i, 23%, $n = 13$; j, 67%, $n = 12$). (e, f) Overexpression of *mHip1* results in reduction and lateral shift of *Dlx3* (black arrows, 43%, $n = 14$). (k, l) Expression of *Dlx3* in ectoderm surrounding the neural plate is increased after *Shh* injection (black arrows, 36%, $n = 14$). (B) (a–d) Frontal views of embryos at NF stage 13, injected side to the right. (a) Strong activation of *Six3* upon injection of *dnWnt-8* mRNA (63%, $n = 11$), while *Dlx3* expression is reduced (b, 58%, $n = 12$). XFD overexpression did not alter *Six3* (c, 95%, $n = 9$) or *Dlx3* (d, 100%, $n = 8$) expression significantly. *LacZ* mRNA was co-injected and visualized by red-gal stain. (C) (a–c) BrdU-proliferation assay and (d–f) phospho-histone H3-proliferation assay. Frontal views of embryos at NF stages 14 and 15, respectively. *mHip1* and *Shh* mRNA was injected into one cell of a two-cell stage embryo, injected side to the right. (b, c) *Rx1* expression (red) was monitored to visualize mHip1 and Shh activity (indicated by dashed line). (b, e) The number of BrdU- and p-H3-positive cells is slightly enhanced by *Shh* and reduced upon *mHip1* overexpression (c, f) versus control embryos (a, d). (g–h) Frontal views of tailbud embryos at NF stage 33 after TUNEL staining. (h) *Shh* overexpression reduces cell death, whereas the number of apoptotic cells is increased upon *mHip1* injection (i). *LacZ* mRNA was co-injected as a lineage tracer (light blue). (j–l) Mitotic arrest assay. (j) Control embryo, showing that normal *Rx1* expression is maintained after HUA treatment. (i) *mHip1* injection still expands the retinal territory (71%, $n = 34$), whereas in *Shh* injected embryos *Rx1* expression is reduced (k).

substantially alter the expression of either marker (Figs. 6B, c–d). Thus, we conclude that the increase of anterior neural plate precursor cells upon *mHip1* overexpression is basically achieved through the inhibition of Wnt-8 signaling.

Two possible mechanisms could explain the increased number of retinal precursor cells. First, non-neural ectoderm could become committed toward the retinal program. Second, enhanced proliferation of retinal precursor cells could increase the size of the early eye field. It is important to note that enhanced proliferation would also push the border between neural and non-neural ectoderm laterally. Therefore, it might be impossible to distinguish between transdifferentiation and proliferation merely on the basis of the analysis of cell fate markers. Therefore, we investigated if *mHip1* overexpression also affects cell proliferation. Mitotic activity in *mHip1* mRNA-injected embryos was monitored by BrdU incorporation and by staining for phosphorylated Histone H3 (Figs. 6C, c, f). We observed a slight reduction of BrdU and P-H3 positive cells upon *mHip1* microinjection, while additional Hh, which has been described as a mitogen (Jensen and Wallace, 1997), accordingly increased the number of mitotic cells (Figs. 6C, b, e). Next, we examined the rate of apoptosis, which could also account for differences in eye size. Whereas *mHip1* overexpression led even to an increased rate of apoptosis, *Shh*-injected embryos revealed less apoptotic cells (Figs. 6C, g–i).

If *mHip1* induces an extension of the retinal field by the stimulation of cell proliferation, mitotic inhibitors such as hydroxyurea/aphidicolin (HUA) (Harris and Hartenstein, 1991) should block it. However, HUA treatment will not block the enlargement of the eye field by *mHip1* if primarily cell fate is regulated but not cell proliferation (Coffman et al., 1993). In fact, the expansion of the eye field, as monitored by *Rx1* expression in early neurula (NF stage 14), was still observed in *mHip1*-injected, HUA-treated embryos, but not in control embryos (Figs. 6C, j, l). Furthermore, we still observed a reduction of *Rx1* expression upon *Shh* mRNA injection in HUA-treated embryos, which identifies Shh as a cell fate regulator as reported before (Fig. 6C, k; Ericson et al., 1997). Taken together, our results suggest that the enlargement of the eye, as induced by *Hip* overexpression, is primarily caused by a fate change of the neural and non-neural ectoderm toward the retinal program and not by increased mitotic activity.

Specific suppression of Xhip function

To further investigate the function of *Xhip* during early patterning of the anterior neuroectoderm, we microinjected a morpholino oligonucleotide directed against *Xhip* mRNA (Xhip-M) that specifically blocks translation of the corresponding protein. We focused on the olfactory and lens placodes, which both express *Xhip*. To trace the fate of the olfactory placodes, we monitored the expression of *Emx2*, whose transcripts were also found in the telencephalon and the branchial arches (Pannese et al., 1998). To follow the fate of the lens placode, we examined the expression of *Pitx3*, which is a marker for the lens epithelium (Pommereit et al., 2001). Furthermore, we investigated the expression of the segment-specific hindbrain marker gene *Krox-20* and of *En-2* as a marker for the midbrain–hindbrain boundary in combination with *Emx2* to check for shifts of the anterior–posterior axis. In *Xhip*-morpholino-injected embryos, the expression of *Emx2* was specifically suppressed within the olfactory placodes and branchial arches. In both structures, the level of *Emx2* transcription was absent or strongly reduced, whereas *Emx2* expression in the telencephalon was not altered (Figs. 7b–d). Likewise, the segmental expression of *Krox-20* and of *En-2* was not changed, which indicated that the *Xhip*-morpholino did not interfere with anterior–posterior neural patterning (Figs. 7a–d). Furthermore, *Xpitx3* expression in the lens placode was absent upon the injection of an *Xhip*-morpholino, but was still detected in the head mesenchyme (Figs. 7f–h). Interestingly, the loss of lens tissue coincides with the formation of a malformed retina and the loss of the retinal pigment epithelium (Figs. 7d, h, l). However, the level of *Rx1* expression was not reduced (Figs. 7k, l), similar to what has been reported in mice in respect to a lens-specific *Pax6* mutant (Ashery-Padan et al., 2000). The microinjection of *mHip1* mRNA resulted in the formation of multiple otic vesicles, as we had reported before (Koebernick et al., 2003), although *Xhip* is not expressed during otic vesicle formation. However, we analyzed the expression of *Pax2* in *Xhip*-morpholino-injected embryos. Interestingly, in none of the injected embryos (100%, $n = 47$) were we able to detect a reduction of *Pax2* expression, but the typical reduction of RPE formation upon *Xhip*-morpholino was clearly visible (Figs. 7o, p).

To further test the specificity of the *Xhip*-morpholino, we rescued the resulting phenotype by the co-injection of small increasing amounts of *mHip1* RNA, which was not targeted by the *Xhip*-morpholino (Fig. 7r). We could not inject higher amounts of rescue mRNA because the embryos started to develop the overexpression phenotype. In addition, the injection of a standard control morpholino oligonucleotide (Contr-M) did not cause any malformations (Figs. 7e, i, m, q). Thus, the inactivation of *Xhip* function resulted in a specific suppression of marker genes of the olfactory and lens placodes, where endogenous *Xhip* is expressed, but did not alter the expression of these marker genes in non-overlapping regions.

Discussion

The microinjection of *Hip* mRNA resulted in an enormous enlargement of distal eye structures and of the olfactory placode, whereas the suppression of Xhip function by means of antisense morpholinos resulted in a suppression of olfactory and lens placode formation and a mild reduction of retinal tissue in *Xenopus*. In addition to the described

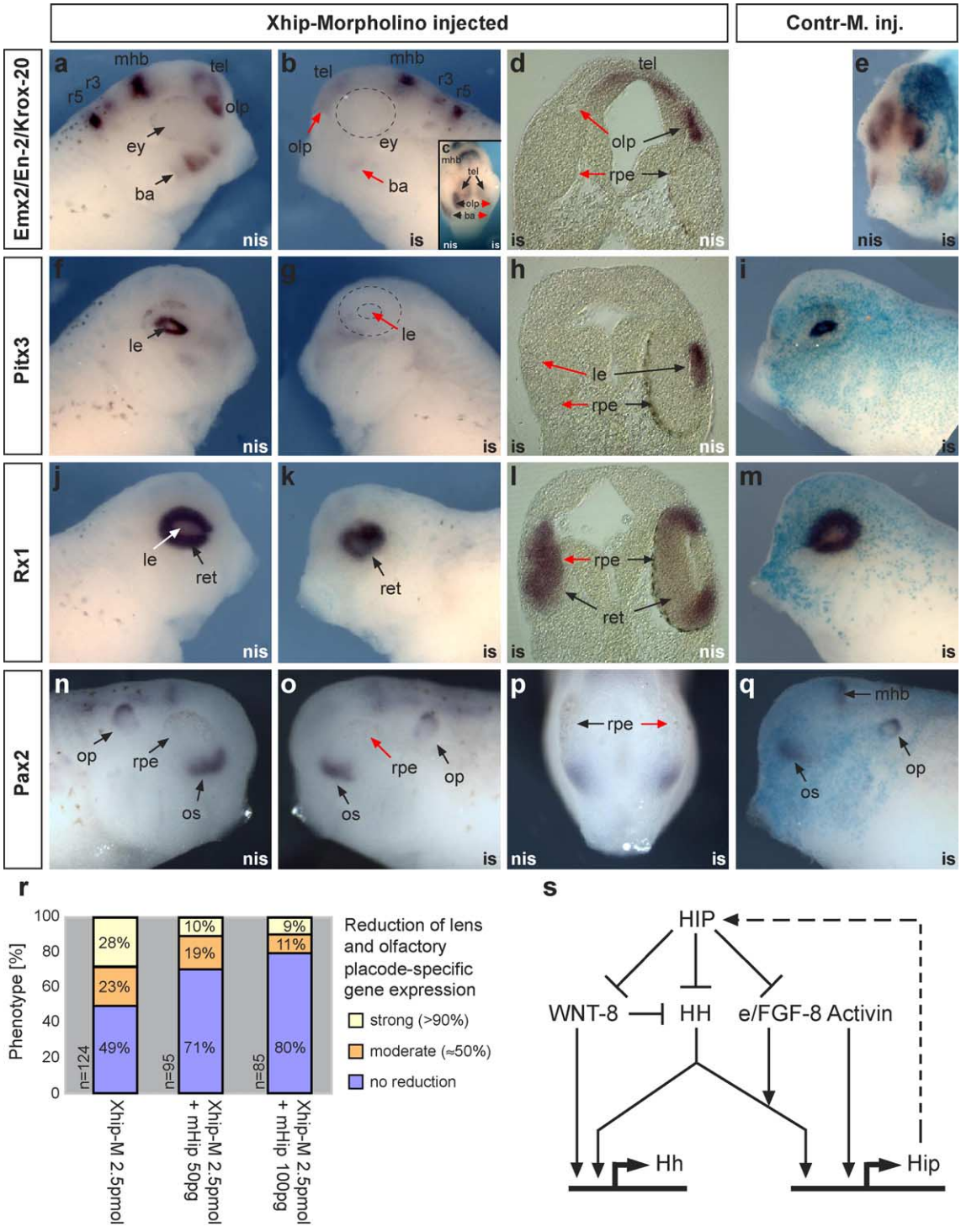

Fig. 7. Suppression of *Xhip* function by antisense-morpholino injection resulted in loss of lens and olfactory placode formation. Whole mount in situ hybridization of *Xhip*-morpholino (a–d, f–h, j–l, n–p) and control-morpholino (e, i, m, q) injected embryos at NF stage 36. (a, f, j, n) Lateral anterior view of the non-injected side. (c, e) Frontal view, injected side to the right. (d, h, l) Horizontal vibratome sections of the corresponding embryos. In control-morpholino (5 pmol) injected embryos *LacZ* mRNA was co-injected as a lineage tracer (light blue). (a–c) Expression of *Krox-20*, *En-2* and *Emx2* was detected simultaneously. (b, c, d) *Xhip*-morpholino injection into one cell of a two cell-stage embryo (2.5 pmol/blastomere) did suppress the expression of *Emx2* in the olfactory placode and branchial arches (74%, $n = 31$; red arrows), and that of *Xpitx3* in the lens ectoderm (65%, $n = 40$; red arrow in g, h). (k, l) The expression level of *Rx1* in the remaining eye cup was not altered, although the morphology of the eye cup was perturbed and the retinal pigment epithelium was not formed (68%, $n = 38$; d, h, l). (n–p) *Xhip*-morpholino injection did not suppress otic vesicle formation as shown by *Pax2* expression, but RPE formation (100%, $n = 47$; red arrows in o, p). (r) Increasing amounts of *mHip1* mRNA (50 or 100 pg) injected together with *Xhip* morpholino rescued the formation of lens and olfactory placodes. (s) Summary diagram of interactions of Hip, Hh, Wnt-8, Fgf-8 and activin. The arrows do not suggest direct interactions; for details, see Discussion. Abbreviations: ba, branchial arches; ey, eye; is, injected site; le, lens; mhb, midbrain–hindbrain boundary; nis, non-injected side; olp, olfactory placode; op, otic vesicle; os, optic stalk; r3/5, rhombomere 3/5; ret, retina; rpe, retinal pigment epithelium; tel, telencephalon.

activity of *mHip1* as a Hedgehog-specific antagonist in mice (Chuang and McMahon, 1999), we identified *mHip1* as an inhibitor of Fgf (eFgf/Fgf-8) and Wnt-8 signaling. We conclude that distinct sensorial placodes are specified under the influence of certain overlapping signaling activities that are controlled by the localized expression of secreted inhibitors, such as the *Hip* protein.

Molecular mechanism of Hip activities

In a previous study, murine Hip1 has been described as a type-I transmembrane protein that can bind to and inhibits the activity of all mammalian Hh proteins (Chuang and McMahon, 1999). Our results are consistent with this observation, since the induction of the Hh target *Ptch1* by *Xshh* was inhibited by mHip1 in neuralized explants. In addition, with eFgf/Fgf-8 and Wnt-8, we were able to identify two other signaling pathways that were blocked by mHip1. In contrast to Hh proteins, mHip1 exhibits specificity with respect to Wnts. We found that the activity of Wnt-8 but not of Wnt-3a was suppressed by mHip1. Similarly, Frzb-1 has been reported to block Wnt-1 and Wnt-8 signaling but not that of Wnt-3a (Wang et al., 1997a). As negative-feedback regulators in the Fgf pathway, only *sprouty2/4* and *sef* have been described, which act downstream of the receptor (Furthauer et al., 2002; Hanafusa et al., 2002; Tsang et al., 2002). In contrast, Hip is expressed independently of Fgf signals and acts most likely at the level or upstream of the receptor, since Elk rescued eFgf activity in the presence of mHip1, and a non-membrane bound form of mHip1 (HipΔC22) still interferes with Fgf signaling (data not shown).

Like *Ptc1*, *Hip1* expression is activated by *Shh* in the mouse and, as demonstrated here, in *Xenopus* embryos. In animal cap explants, we found that Shh and Wnt-8 can both induce *Xhip* in the absence of BMP signals. A comparable negative feedback loop has been described in the context of somite development, where Shh was found to up-regulate *secreted frizzled related protein* (*2Sfrp2*), which encodes a potential Wnt antagonist (Lee et al., 2000). Likewise, Wnt4 can induce *growth arrest specific gene 1* (*Gas1*) that antagonizes Shh (Lee et al., 2001). We found that Fgf signals can enhance the induction of *Shh* but not of *Xhip* mediated by *Shh* in neuralized explants. These results are in agreement with what has been reported in mice, where Fgf-8 is needed to maintain *Shh* expression in the context of limb development (Lewandoski et al., 2000). Interestingly, we found that Wnt-8 was able to induce *Xhip* but suppressed the concurrent auto-induction of *Shh*, indicating that Wnt signals act independently from Shh to induce *Xhip* expression. In contrast to Hh and Wnt-8, activin was found to be sufficient to induce *Xhip* expression (Yokotal et al., 1995). Inside the cell, activin and BMP signals are mediated by Smad2/3 and Smad1/5/8. The Smads compete for a limited pool of Smad4, which is shared between the pathways (Shi and Massague, 2003). Therefore, the application of activin in the animal cap system results indirectly in an intracellular suppression of BMP signals (Candia et al., 1997), which may induce *Xhip* as a consequence of *Shh* expression by dorsalizing Smads (Takabatake et al., 1996). Thus, *Xhip* expression is regulated by the integration of a complex signaling network, of which the activity of extracellular components is regulated via a negative feedback loop through their interaction with Hip (Fig. 7s).

Role of Shh, Wnt, and Fgf signals in the patterning of the anterior neural plate

Shh has been described in chicken and *Xenopus* as a key regulator for the splitting of the eye field, which coincides with the establishment of the proximo-distal axes of the eye anlagen (Li et al., 1997; Pera and Kessel, 1997). Shh-promoted ventral retinal cell fates at the expense of dorsal or distal retinal cell fates in zebrafish and *Xenopus*, such as photoreceptors (Hallonet et al., 1999; Macdonald et al., 1995). In contrast, the inhibition of Hh signaling by cyclopamine resulted in a holoprosencephalic-like (HPE) phenotype and promoted neuro-retinal cell fates, but did not increase the size of the remaining retinal tissue (Perron et al., 2003; Take-uchi et al., 2003 and Supplementary Fig. 2a). In line with these reports, the overexpression of *mHip1* or *Xhip* also promoted neuro-retinal cell fates, but led to enlarged eye-like structures. Furthermore, within the *Hip*-injected eye, we found dispersed photoreceptor cells, a finding which is in agreement to what has been reported in mice, where the conditional loss of *Shh* in ganglion cells interfered with the proper stratification of the retina (Dakubo et al., 2003).

In amphibian and chicken embryos, Fgf and Wnt signals had previously been identified as posteriorizing molecules, which were able to induce posterior neural markers at the expense of anterior marker gene expression in early embryogenesis (Amaya et al., 1993; Lamb and Harland, 1995; McGrew et al., 1997). Microinjections of high amounts of *eFgf/Fgf-8* mRNA completely suppress the development of anterior structures in the frog, whereas low amounts of *eFgf/Fgf-8* specifically block eye formation (Christen and Slack, 1997; Isaacs et al., 1994). In *Xenopus*, all known FGF receptors (*Fgfr1* to *Fgfr4*) are expressed in overlapping areas within the presumptive head region at high levels, while a low level expression was detected in all other tissues (Hongo et al., 1999). The injection of a dominant-negative version of *Xfgfr-4a* has been reported to result in reduction of head structures, although cement glands were expanded (Hongo et al., 1999). Consistent with the view that FGF-8 acts through FGFR1 in the developing forebrain (Hebert et al., 2003; Ornitz et al., 1996), we show that the repression of Fgf signaling by *dnFgfr1* (XFD) resulted in enlarged retinal structures (Figs. 5B, d′–d″ and Supplementary Fig. 2c). Moreover, overexpression of a dominant negative Ras mutant, in addition to XFD, blocked

the expression of *Sox2* in the posterior neural plate, but did not interfere with the induction of anterior neural markers by noggin or neurogenin (Ribisi et al., 2000). However, the repression of posterior neural development upon XFD injection may explain the mild enlargement of the anterior structures we observed due to the loss of a posterior signal that either promotes posterior and/or represses anterior development.

Several lines of evidence point to the fact that the ectopic expression of members of the canonical Wnt pathway, or of Wnt inhibitors, inhibits or promotes head development, respectively (Glinka et al., 1997; Hoppler et al., 1996), whereas the induction of ectopic eyes by the Wnt receptor Xfz3 depends on the non-canonical cell polarity pathway (Rasmussen et al., 2001). Moreover, the induction of ectopic eyes by IGF is partly mediated by an inhibition of β-catenin dependent Wnt-activity (Pera et al., 2001; Richard-Parpaillon et al., 2002), and a mutation in the zebrafish Masterblind/Axin1 gene, which results in stabilization of β-catenin, led to a fate transformation of telencephalon and eyes to diencephalon (Heisenberg et al., 2001). In line with this observation, the specific inhibition of Wnt-8 by dnWnt-8 led to a striking enlargement of the eye (Supplementary Fig. 2d). Similarly, the knock-down of *Wnt-8* by antisense morpholinos in zebrafish was reported to result in an expansion of the eye primordium, as marked by *Six3* expression (Kim et al., 2002). Thus, the generation of giant eye-like structures by *Hip* overexpression resembles primarily a repression of Wnt-8 and partially of FGF signaling. The contribution of Shh in this respect remains to be elucidated, although the modulation of Shh signaling clearly directed cell fate decisions within the eye field, without a major impact on the eye size.

Role of Xhip in placode development

In early development, *Xhip*-positive cells were not identified within the region of the anterior neural plate until neurulation. Although *Hip* overexpression resulted in a strong activation of the retinal fate within the prospective forebrain, its endogenous expression is not directly essential for the normal development of the retina. In fact, our experiments show that loss of *Xhip* function led to an inhibition of olfactory and lens formation, which in turn impaired the morphogenesis of the eye cup. The influence of the lens on the forming retina has been reported after mechanical or genetic ablation of the lens (Ashery-Padan et al., 2000; Breitman et al., 1989; Coulombre and Coulombre, 1964; Harrington et al., 1991; Kaur et al., 1989). In all cases, the sensory retina was highly convoluted, while the stratification of the retina itself and the formation of retinal pigment epithelium were almost normal. Moreover, the eyeless form of the cave fish *Astyanax mexicanus* restored an eye when the lens ectoderm of the eyed surface form was transplanted. (Yamamoto and Jeffery, 2000). Candidate molecules responsible for this process are FGF1 and 2, which are highly expressed in the lens ectoderm (McAvoy et al., 1991; Pittack et al., 1997). Fgf signaling can induce neural retina differentiation (Govindarajan and Overbeek, 2001; Lovicu and Overbeek, 1998), while it may not be necessary for the formation of the optic cup from the optic vesicle (Hyer et al., 1998). Beyond their function in differentiation, Fgf signals seem to provide positional information regarding pattern formation of the neural retina and guide the distinction between neural retina and pigmented epithelium (Sakaguchi et al., 1997). This was further illustrated by the finding that the early removal of lens ectoderm, which is a rich source of Fgf, led to disorganized optic vesicles (Hyer et al., 2003), as shown for the *Hip* overexpression. Still it is not clear if Fgf signaling contributes already to the induction of the presumptive lens ectoderm (Hirsch and Grainger, 2000). A target of Fgf signaling in the lens placode is *Pax6*, which is able to induce ectopic lens formation in *Xenopus* embryos (Altmann et al., 1997) and is required in the lens ectoderm of murine embryos for lens formation (Ashery-Padan et al., 2000). The giant retina induced by *Hip* overexpression showed impaired stratification, which confirms that positional information, provided by certain signaling molecules, is needed to establish the layering within the developing eye. *Xhip* is expressed in the presumptive lens epithelium at an embryonic stage before the lens placode is specified and is still responsive to Hh signals (Koebernick et al., 2001). Consistent with the role of Hip as an Hh inhibitor, it may function to block long-range acting Hh-molecules emanating from the prechordal plate. Otherwise, these Hh molecules may interfere with lens specification within the presumptive lens epithelium, as shown by the overexpression of Hh, which strongly inhibits lens formation.

In the olfactory placode, *Pax6* expression has also been reported to depend on Fgf signals. The disruption of Fgf signaling in the telencephalon and the olfactory epithelium led to malformed olfactory bulbs, similar to what has been recently described in Small-eye (*Sey*) mice (Dellovade et al., 1998; Lopez-Mascaraque et al., 1998). Thus, during the development of the eye and the nose, Pax6 function depends on Fgf signals, which may also provide positional information for the formation of both organs.

Much less is known about the contribution of Wnt signals in respect to lens and olfactory development. However, Wnt signals contribute to the differentiation of cranial placodes, since different components of the Wnt signaling pathways are expressed in corresponding regions during development (Esteve et al., 2000; Finley et al., 2003; Stark et al., 2000) and a mutation in the zebrafish Masterblind/Axin1 gene is also characterized by the absence of olfactory placodes (Heisenberg et al., 2001; van de Water et al., 2001). More recently, it has been shown in LRP6-deficient mice that lens epithelial cells, which were also found to express Wnt2b in avian embryos, depend on Wnt/β-catenin signals. These signals are most likely required for

the regulation of cell division in the lens epithelium and are important for the distinction between differentiating elongated fiber cells at the edge of the lens epithelium and lens stem cells within the lens epithelium (Jasoni et al., 1999; Stark et al., 2000; Stump et al., 2003). Similarly, Wnt/β-Catenin has been identified as a positive regulator for the induction of the neural crest and for the specification of sensory neurons derived from the neural crest in murine and chicken embryos (Garcia-Castro et al., 2002; Hari et al., 2002; Lee et al., 2004). Thus, Wnt/β-Catenin may provide a function in the control of fate decisions in early neural crest development and, more generally, with respect to cells that are derived from the preplacodal ectoderm field. Consistent with this, the interference with proper Wnt function by the microinjection of Hip morpholinos was found to inhibit the specification of lens and olfactory placodes.

Previously, we have reported that the repression of Hh signaling by overexpression of *mHip1* or a dominant negative form of the Hh receptor *XPtc1* (XPtc1ΔLoop2), respectively, as well as the activation of Hh signaling by overexpression of *XSmo* resulted in the induction of multiple otic vesicles in tadpole stage embryos and of the general placodal marker genes *Eya1* during early neurulation (Koebernick et al., 2003). This puzzling result was explained by a scenario in which a certain level of active Hh signaling is required for the induction of otic placode identity. Since we demonstrated that *mHip1* also interferes with Wnt and Fgf signals, it is conceivable that the integration of all three signaling pathways determines otic specification. Thus, the induction of ectopic otic vesicles in chicken by Fgf3 (Vendrell et al., 2000) in zebrafish by Fgf3/Fgf8 (Phillips et al., 2004) and in *Xenopus* embryos treated with lithium (Gutknecht and Fritzsch, 1990) or Hh antagonists and agonists, might result from a joint influence on GSK-3 activity (Holnthoner et al., 2002; Israsena et al., 2004; Klein and Melton, 1996), which is an important intracellular mediator of all three signaling pathways (Doble and Woodgett, 2003).

Therefore, we propose that Hip is a multifunctional antagonist, which is important in shielding cells or tissues from excess or aberrant activities of distinct signaling molecules, but these molecules, on the other hand, may positively regulate the expression of Hip.

Acknowledgments

We thank A.W. Brändli for Pax2, E.M. De Robertis for Chordin, R.M. Harland for Otx2, M. Jamrich for *Xrx1*, A.P. McMahon for *mHip1*, W. Knöchel for BMP4, R.T. Moon for Shh, dnWnt-8, N. Papalopulu for Dlx3, R.A. Rupp for pCS2+, G. Schlosser for help with the placodal morphology, J.M. Slack for eFgf, J.C. Smith for Xbra, J. Wittbrodt for activin. This work was supported by a fund from the Deutsche Forschungsgemeinschaft to T.H. (SFB 271).

Appendix A. Supplementary data

Supplementary data associated with this article can be found, in the online version, at doi:10.1016/j.ydbio.2004.09.016.

References

Altmann, C.R., Chow, R.L., Lang, R.A., Hemmati-Brivanlou, A., 1997. Lens induction by Pax-6 in *Xenopus laevis*. Dev. Biol. 185, 119–123.

Amato, M.A., Boy, S., Perron, M., 2004. Hedgehog signaling in vertebrate eye development: a growing puzzle. Cell. Mol. Life Sci. 61, 899–910.

Amaya, E., Stein, P.A., Musci, T.J., Kirschner, M.W., 1993. FGF signaling in the early specification of mesoderm in *Xenopus*. Development 118, 477–487.

Ashery-Padan, R., Marquardt, T., Zhou, X., Gruss, P., 2000. Pax6 activity in the lens primordium is required for lens formation and for correct placement of a single retina in the eye. Genes Dev. 14, 2701–2711.

Baker, C.V., Bronner-Fraser, M., 2001. Vertebrate cranial placodes I. Embryonic induction. Dev. Biol. 232, 1–61.

Baker, J.C., Beddington, R.S., Harland, R.M., 1999. Wnt signaling in *Xenopus* embryos inhibits bmp4 expression and activates neural development. Genes Dev. 13, 3149–3159.

Bell, E., Munoz-Sanjuan, I., Altmann, C.R., Vonica, A., Brivanlou, A.H., 2003. Cell fate specification and competence by Coco, a maternal BMP, TGFbeta and Wnt inhibitor. Development 130, 1381–1389.

Bernier, G., Panitz, F., Zhou, X., Hollemann, T., Gruss, P., Pieler, T., 2000. Expanded retina territory by midbrain transformation upon overexpression of Six6 (Optx2) in *Xenopus* embryos. Mech. Dev. 93, 59–69.

Breitman, M.L., Bryce, D.M., Giddens, E., Clapoff, S., Goring, D., Tsui, L.C., Klintworth, G.K., Bernstein, A., 1989. Analysis of lens cell fate and eye morphogenesis in transgenic mice ablated for cells of the lens lineage. Development 106, 457–463.

Briscoe, J., Pierani, A., Jessell, T.M., Ericson, J., 2000. A homeodomain protein code specifies progenitor cell identity and neuronal fate in the ventral neural tube. Cell 101, 435–445.

Candia, A.F., Watabe, T., Hawley, S.H., Onichtchouk, D., Zhang, Y., Derynck, R., Niehrs, C., Cho, K.W., 1997. Cellular interpretation of multiple TGF-beta signals: intracellular antagonism between activin/BVg1 and BMP-2/4 signaling mediated by Smads. Development 124, 4467–4480.

Chow, R.L., Lang, R.A., 2001. Early eye development in vertebrates. Annu. Rev. Cell Dev. Biol. 17, 255–296.

Christen, B., Slack, J.M., 1997. FGF-8 is associated with anteroposterior patterning and limb regeneration in *Xenopus*. Dev. Biol. 192, 455–466.

Chuang, P.T., McMahon, A.P., 1999. Vertebrate Hedgehog signaling modulated by induction of a Hedgehog-binding protein. Nature 397, 617–621.

Chuang, J.C., Mathers, P.H., Raymond, P.A., 1999. Expression of three Rx homeobox genes in embryonic and adult zebrafish. Mech. Dev. 84, 195–198.

Chuang, P.T., Kawcak, T., McMahon, A.P., 2003. Feedback control of mammalian Hedgehog signaling by the Hedgehog-binding protein, Hip1, modulates Fgf signaling during branching morphogenesis of the lung. Genes Dev. 17, 342–347.

Coffman, C.R., Skoglund, P., Harris, W.A., Kintner, C.R., 1993. Expression of an extracellular deletion of Xotch diverts cell fate in *Xenopus* embryos. Cell 73, 659–671.

Coulombre, A.J., Coulombre, J.L., 1964. Lens development: I. Role of the lens in eye growth. J. Exp. Zool. 156, 39–47.

Crossley, P.H., Martinez, S., Ohkubo, Y., Rubenstein, J.L., 2001. Coordinate expression of Fgf8, Otx2, Bmp4, and Shh in the rostral prosencephalon during development of the telencephalic and optic vesicles. Neuroscience 108, 183–206.

Curran, K.L., Grainger, R.M., 2000. Expression of activated MAP kinase in *Xenopus laevis* embryos: evaluating the roles of FGF and other signaling pathways in early induction and patterning. Dev. Biol. 228, 41–56.

Dakubo, G.D., Wang, Y.P., Mazerolle, C., Campsall, K., McMahon, A.P., Wallace, V.A., 2003. Retinal ganglion cell-derived sonic hedgehog signaling is required for optic disc and stalk neuroepithelial cell development. Development 130, 2967–2980.

Dellovade, T.L., Pfaff, D.W., Schwanzel-Fukuda, M., 1998. Olfactory bulb development is altered in small-eye (Sey) mice. J. Comp. Neurol. 402, 402–418.

Doble, B.W., Woodgett, J.R., 2003. GSK-3: tricks of the trade for a multi-tasking kinase. J. Cell Sci. 116, 1175–1186.

Eagleson, G.W., Harris, W.A., 1990. Mapping of the presumptive brain regions in the neural plate of *Xenopus laevis*. J. Neurobiol. 21, 427–440.

Eagleson, G., Ferreiro, B., Harris, W.A., 1995. Fate of the anterior neural ridge and the morphogenesis of the *Xenopus* forebrain. J. Neurobiol. 28, 146–158.

Ekker, S.C., Ungar, A.R., Greenstein, P., von Kessler, D.P., Porter, J.A., Moon, R.T., Beachy, P.A., 1995. Patterning activities of vertebrate hedgehog proteins in the developing eye and brain. Curr. Biol. 5, 944–955.

Enwright III, J.F., Grainger, R.M., 2000. Altered retinoid signaling in the heads of small eye mouse embryos. Dev. Biol. 221, 10–22.

Ericson, J., Muhr, J., Jessell, T.M., Edlund, T., 1995. Sonic hedgehog: a common signal for ventral patterning along the rostrocaudal axis of the neural tube. Int. J. Dev. Biol. 39, 809–816.

Ericson, J., Rashbass, P., Schedl, A., Brenner-Morton, S., Kawakami, A., van Heyningen, V., Jessell, T.M., Briscoe, J., 1997. Pax6 controls progenitor cell identity and neuronal fate in response to graded Shh signaling. Cell 90, 169–180.

Esteve, P., Morcillo, J., Bovolenta, P., 2000. Early and dynamic expression of cSfrp1 during chick embryo development. Mech. Dev. 97, 217–221.

Finley, K.R., Tennessen, J., Shawlot, W., 2003. The mouse secreted frizzled-related protein 5 gene is expressed in the anterior visceral endoderm and foregut endoderm during early post-implantation development. Gene Expr. Patterns 3, 681–684.

Furthauer, M., Lin, W., Ang, S.L., Thisse, B., Thisse, C., 2002. Sef is a feedback-induced antagonist of Ras/MAPK-mediated FGF signaling. Nat. Cell Biol. 4, 170–174.

Furuta, Y., Hogan, B.L., 1998. BMP4 is essential for lens induction in the mouse embryo. Genes Dev. 12, 3764–3775.

Garcia-Castro, M.I., Marcelle, C., Bronner-Fraser, M., 2002. Ectodermal Wnt function as a neural crest inducer. Science 297, 848–851.

Glinka, A., Wu, W., Onichtchouk, D., Blumenstock, C., Niehrs, C., 1997. Head induction by simultaneous repression of Bmp and Wnt signaling in *Xenopus*. Nature 389, 517–519.

Gomez-Skarmeta, J., de La Calle-Mustienes, E., Modolell, J., 2001. The Wnt-activated Xiro1 gene encodes a repressor that is essential for neural development and downregulates Bmp4. Development 128, 551–560.

Govindarajan, V., Overbeek, P.A., 2001. Secreted FGFR3, but not FGFR1, inhibits lens fiber differentiation. Development 128, 1617–1627.

Grainger, R.M., 1992. Embryonic lens induction: shedding light on vertebrate tissue determination. Trends Genet. 8, 349–355.

Gutknecht, D., Fritzsch, B., 1990. Lithium can transform ear placodes of *Xenopus* into multiple otic vesicles connected by tubes. Naturwissenschaften 77, 235–237.

Hallonet, M., Hollemann, T., Pieler, T., Gruss, P., 1999. Vax1, a novel homeobox-containing gene, directs development of the basal forebrain and visual system. Genes Dev. 13, 3106–3114.

Hanafusa, H., Torii, S., Yasunaga, T., Nishida, E., 2002. Sprouty1 and Sprouty2 provide a control mechanism for the Ras/MAPK signaling pathway. Nat. Cell Biol. 4, 850–858.

Hari, L., Brault, V., Kleber, M., Lee, H.Y., Ille, F., Leimeroth, R., Paratore, C., Suter, U., Kemler, R., Sommer, L., 2002. Lineage-specific requirements of beta-catenin in neural crest development. J. Cell Biol. 159, 867–880.

Harland, R., 2000. Neural induction. Curr. Opin. Genet. Dev. 10, 357–362.

Harrington, L., Klintworth, G.K., Secor, T.E., Breitman, M.L., 1991. Developmental analysis of ocular morphogenesis in alpha A-crystallin/diphtheria toxin transgenic mice undergoing ablation of the lens. Dev. Biol. 148, 508–516.

Harris, W.A., Hartenstein, V., 1991. Neuronal determination without cell division in *Xenopus* embryos. Neuron 6, 499–515.

Hebert, J.M., Lin, M., Partanen, J., Rossant, J., McConnell, S.K., 2003. FGF signaling through FGFR1 is required for olfactory bulb morphogenesis. Development 130, 1101–1111.

Heisenberg, C.P., Houart, C., Take-Uchi, M., Rauch, G.J., Young, N., Coutinho, P., Masai, I., Caneparo, L., Concha, M.L., Geisler, R., Dale, T.C., Wilson, S.W., Stemple, D.L., 2001. A mutation in the Gsk3-binding domain of zebrafish Masterblind/Axin1 leads to a fate transformation of telencephalon and eyes to diencephalon. Genes Dev. 15, 1427–1434.

Hensey, C., Gautier, J., 1998. Programmed cell death during *Xenopus* development: a spatio-temporal analysis. Dev. Biol. 203, 36–48.

Hirsch, N., Grainger, R.M., 2000. Induction of the lens. Results Probl. Cell Differ. 31, 51–68.

Hirsch, N., Harris, W.A., 1997. *Xenopus* Pax-6 and retinal development. J. Neurobiol. 32, 45–61.

Hollemann, T., Pieler, T., 1999. Xpitx-1: a homeobox gene expressed during pituitary and cement gland formation of *Xenopus* embryos. Mech. Dev. 88, 249–252.

Hollemann, T., Bellefroid, E., Pieler, T., 1998. The *Xenopus* homologue of the *Drosophila* gene tailless has a function in early eye development. Development 125, 2425–2432.

Hollemann, T., Panitz, F., Pieler, T., 1999. In situ hybridization techniques with *Xenopus* embryos. In: Richter, J.D. (Ed.), A Comparative Methods Approach to the Study of Oocytes and Embryos. Oxford Univ. Press, New York, pp. 279–290.

Holnthoner, W., Pillinger, M., Groger, M., Wolff, K., Ashton, A.W., Albanese, C., Neumeister, P., Pestell, R.G., Petzelbauer, P., 2002. Fibroblast growth factor-2 induces Lef/Tcf-dependent transcription in human endothelial cells. J. Biol. Chem. 277, 45847–45853.

Hongo, I., Kengaku, M., Okamoto, H., 1999. FGF signaling and the anterior neural induction in *Xenopus*. Dev. Biol. 216, 561–581.

Hoppler, S., Brown, J.D., Moon, R.T., 1996. Expression of a dominant-negative Wnt blocks induction of MyoD in *Xenopus* embryos. Genes Dev. 10, 2805–2817.

Hsieh, J.C., Kodjabachian, L., Rebbert, M.L., Rattner, A., Smallwood, P.M., Samos, C.H., Nusse, R., Dawid, I.B., Nathans, J., 1999. A new secreted protein that binds to Wnt proteins and inhibits their activities. Nature 398, 431–436.

Hyatt, G.A., Schmitt, E.A., Marsh-Armstrong, N., McCaffery, P., Drager, U.C., Dowling, J.E., 1996. Retinoic acid establishes ventral retinal characteristics. Development 122, 195–204.

Hyer, J., Mima, T., Mikawa, T., 1998. FGF1 patterns the optic vesicle by directing the placement of the neural retina domain. Development 125, 869–877.

Hyer, J., Kuhlman, J., Afif, E., Mikawa, T., 2003. Optic cup morphogenesis requires pre-lens ectoderm but not lens differentiation. Dev. Biol. 259, 351–363.

Ingham, P.W., McMahon, A.P., 2001. Hedgehog signaling in animal development: paradigms and principles. Genes Dev. 15, 3059–3087.

Isaacs, H.V., Pownall, M.E., Slack, J.M., 1994. eFGF regulates Xbra expression during *Xenopus* gastrulation. EMBO J. 13, 4469–4481.

Ishibashi, S., Yasuda, K., 2001. Distinct roles of maf genes during *Xenopus* lens development. Mech. Dev. 101, 155–166.

Israsena, N., Hu, M., Fu, W., Kan, L., Kessler, J.A., 2004. The presence of FGF2 signaling determines whether beta-catenin exerts effects on proliferation or neuronal differentiation of neural stem cells. Dev. Biol. 268, 220–231.

Janknecht, R., Ernst, W.H., Pingoud, V., Nordheim, A., 1993. Activation of ternary complex factor Elk-1 by MAP kinases. EMBO J. 12, 5097–5104.

Jasoni, C., Hendrickson, A., Roelink, H., 1999. Analysis of chicken Wnt-13 expression demonstrates coincidence with cell division in the developing eye and is consistent with a role in induction. Dev. Dyn. 215, 215–224.

Jensen, A.M., Wallace, V.A., 1997. Expression of Sonic hedgehog and its putative role as a precursor cell mitogen in the developing mouse retina. Development 124, 363–371.

Jeon, H., Meng, W., Takagi, J., Eck, M.J., Springer, T.A., Blacklow, S.C., 2001. Implications for familial hypercholesterolemia from the structure of the LDL receptor YWTD-EGF domain pair. Nat. Struct. Biol. 8, 499–504.

Kaur, S., Key, B., Stock, J., McNeish, J.D., Akeson, R., Potter, S.S., 1989. Targeted ablation of alpha-crystallin-synthesizing cells produces lens-deficient eyes in transgenic mice. Development 105, 613–619.

Kenyon, K.L., Moody, S.A., Jamrich, M., 1999. A novel fork head gene mediates early steps during *Xenopus* lens formation. Development 126, 5107–5116.

Kim, S.H., Shin, J., Park, H.C., Yeo, S.Y., Hong, S.K., Han, S., Rhee, M., Kim, C.H., Chitnis, A.B., Huh, T.L., 2002. Specification of an anterior neuroectoderm patterning by Frizzled8a-mediated Wnt8b signaling during late gastrulation in zebrafish. Development 129, 4443–4455.

Klein, P.S., Melton, D.A., 1996. A molecular mechanism for the effect of lithium on development. Proc. Natl. Acad. Sci. U. S. A. 93, 8455–8459.

Koebernick, K., Hollemann, T., Pieler, T., 2001. Molecular cloning and expression analysis of the Hedgehog receptors XPtc1 and XSmo in *Xenopus laevis*. Mech. Dev. 100, 303–308.

Koebernick, K., Hollemann, T., Pieler, T., 2003. A restrictive role for Hedgehog signaling during otic specification in *Xenopus*. Dev. Biol. 260, 325–338.

Ladher, R.K., Church, V.L., Allen, S., Robson, L., Abdelfattah, A., Brown, N.A., Hattersley, G., Rosen, V., Luyten, F.P., Dale, L., Francis-West, P.H., 2000. Cloning and expression of the Wnt antagonists Sfrp-2 and Frzb during chick development. Dev. Biol. 218, 183–198.

Lamb, T.M., Harland, R.M., 1995. Fibroblast growth factor is a direct neural inducer, which combined with noggin generates anterior–posterior neural pattern. Development 121, 3627–3636.

Lee, C.S., Buttitta, L.A., May, N.R., Kispert, A., Fan, C.M., 2000. SHH-N upregulates Sfrp2 to mediate its competitive interaction with WNT1 and WNT4 in the somitic mesoderm. Development 127, 109–118.

Lee, C.S., Buttitta, L., Fan, C.M., 2001. Evidence that the WNT-inducible growth arrest-specific gene 1 encodes an antagonist of sonic hedgehog signaling in the somite. Proc. Natl. Acad. Sci. U. S. A. 98, 11347–11352.

Lee, H.Y., Kleber, M., Hari, L., Brault, V., Suter, U., Taketo, M.M., Kemler, R., Sommer, L., 2004. Instructive role of Wnt/beta-catenin in sensory fate specification in neural crest stem cells. Science 303, 1020–1023.

Lekven, A.C., Buckles, G.R., Kostakis, N., Moon, R.T., 2003. Wnt1 and wnt10b function redundantly at the zebrafish midbrain–hindbrain boundary. Dev. Biol. 254, 172–187.

Lewandoski, M., Sun, X., Martin, G.R., 2000. Fgf8 signaling from the AER is essential for normal limb development. Nat. Genet. 26, 460–463.

Li, H., Tierney, C., Wen, L., Wu, J.Y., Rao, Y., 1997. A single morphogenetic field gives rise to two retina primordia under the influence of the prechordal plate. Development 124, 603–615.

Liu, I.S., Chen, J.D., Ploder, L., Vidgen, D., van der Kooy, D., Kalnins, V.I., McInnes, R.R., 1994. Developmental expression of a novel murine homeobox gene (Chx10): evidence for roles in determination of the neuroretina and inner nuclear layer. Neuron 13, 377–393.

Long, J.E., Garel, S., Depew, M.J., Tobet, S., Rubenstein, J.L., 2003. DLX5 regulates development of peripheral and central components of the olfactory system. J. Neurosci. 23, 568–578.

Lopez-Mascaraque, L., Garcia, C., Valverde, F., de Carlos, J.A., 1998. Central olfactory structures in Pax-6 mutant mice. Ann. N. Y. Acad. Sci. 855, 83–94.

Lovicu, F.J., Overbeek, P.A., 1998. Overlapping effects of different members of the FGF family on lens fiber differentiation in transgenic mice. Development 125, 3365–3377.

Macdonald, R., Barth, K.A., Xu, Q., Holder, N., Mikkola, I., Wilson, S.W., 1995. Midline signaling is required for Pax gene regulation and patterning of the eyes. Development 121, 3267–3278.

Mangold, O., 1931. Das Determinationsproblem: III. Das Wirbeltierauge in der Entwicklung und Regeneration. Ergeb. Biol. 7, 1.

Marquardt, T., Pfaff, S.L., 2001. Cracking the transcriptional code for cell specification in the neural tube. Cell 106, 651–654.

Mathers, P.H., Grinberg, A., Mahon, K.A., Jamrich, M., 1997. The Rx homeobox gene is essential for vertebrate eye development. Nature 387, 603–607.

McAvoy, J.W., Chamberlain, C.G., de Iongh, R.U., Richardson, N.A., Lovicu, F.J., 1991. The role of fibroblast growth factor in eye lens development. Ann. N. Y. Acad. Sci. 638, 256–274.

McCaffery, P., Drager, U.C., 1993. Retinoic acid synthesis in the developing retina. Adv. Exp. Med. Biol. 328, 181–190.

McCarthy, R.A., Barth, J.L., Chintalapudi, M.R., Knaak, C., Argraves, W.S., 2002. Megalin functions as an endocytic sonic hedgehog receptor. J. Biol. Chem. 277, 25660–25667.

McGrew, L.L., Hoppler, S., Moon, R.T., 1997. Wnt and FGF pathways cooperatively pattern anteroposterior neural ectoderm in *Xenopus*. Mech. Dev. 69, 105–114.

Munoz-Sanjuan, I., Brivanlou, A.H., 2002. Neural induction, the default model and embryonic stem cells. Nat. Rev., Neurosci. 3, 271–280.

Nieuwkoop, P.D., Faber, J., 1967. Normal Table of *Xenopus laevis* (Daudin). Amsterdam, North Holland.

Northrop, J., Woods, A., Seger, R., Suzuki, A., Ueno, N., Krebs, E., Kimelman, D., 1995. BMP-4 regulates the dorsal–ventral differences in FGF/MAPKK-mediated mesoderm induction in *Xenopus*. Dev. Biol. 172, 242–252.

Ohkubo, Y., Chiang, C., Rubenstein, J.L., 2002. Coordinate regulation and synergistic actions of BMP4, SHH and FGF8 in the rostral prosencephalon regulate morphogenesis of the telencephalic and optic vesicles. Neuroscience 111, 1–17.

Oliver, G., Mailhos, A., Wehr, R., Copeland, N.G., Jenkins, N.A., Gruss, P., 1995. Six3, a murine homologue of the sine oculis gene, demarcates the most anterior border of the developing neural plate and is expressed during eye development. Development 121, 4045–4055.

Ornitz, D.M., Xu, J., Colvin, J.S., McEwen, D.G., MacArthur, C.A., Coulier, F., Gao, G., Goldfarb, M., 1996. Receptor specificity of the fibroblast growth factor family. J. Biol. Chem. 271, 15292–15297.

Oubrie, A., Rozeboom, H.J., Dijkstra, B.W., 1999. Active-site structure of the soluble quinoprotein glucose dehydrogenase complexed with methylhydrazine: a covalent cofactor-inhibitor complex. Proc. Natl. Acad. Sci. U. S. A. 96, 11787–11791.

Pannese, M., Polo, C., Andreazzoli, M., Vignali, R., Kablar, B., Barsacchi, G., Boncinelli, E., 1995. The *Xenopus* homologue of Otx2 is a maternal homeobox gene that demarcates and specifies anterior body regions. Development 121, 707–720.

Pannese, M., Lupo, G., Kablar, B., Boncinelli, E., Barsacchi, G., Vignali, R., 1998. The *Xenopus* Emx genes identify presumptive dorsal telencephalon and are induced by head organizer signals. Mech. Dev. 73, 73–83.

Pera, E.M., Kessel, M., 1997. Patterning of the chick forebrain anlage by the prechordal plate. Development 124, 4153–4162.

Pera, E., Stein, S., Kessel, M., 1999. Ectodermal patterning in the avian embryo: epidermis versus neural plate. Development 126, 63–73.

Pera, E.M., Wessely, O., Li, S.Y., De Robertis, E.M., 2001. Neural and head induction by insulin-like growth factor signals. Dev. Cell 1, 655–665.

Pera, E.M., Ikeda, A., Eivers, E., De Robertis, E.M., 2003. Integration of IGF, FGF, and anti-BMP signals via Smad1 phosphorylation in neural induction. Genes Dev. 17, 3023–3028.

Perron, M., Boy, S., Amato, M.A., Viczian, A., Koebernick, K., Pieler, T., Harris, W.A., 2003. A novel function for Hedgehog signaling in retinal pigment epithelium differentiation. Development 130, 1565–1577.

Phillips, B.T., Storch, E.M., Lekven, A.C., Riley, B.B., 2004. A direct

role for Fgf but not Wnt in otic placode induction. Development 131, 923–931.
Pittack, C., Grunwald, G.B., Reh, T.A., 1997. Fibroblast growth factors are necessary for neural retina but not pigmented epithelium differentiation in chick embryos. Development 124, 805–816.
Pommereit, D., Pieler, T., Hollemann, T., 2001. Xpitx3: a member of the Rieg/Pitx gene family expressed during pituitary and lens formation in *Xenopus laevis*. Mech. Dev. 102, 255–257.
Rasmussen, J.T., Deardorff, M.A., Tan, C., Rao, M.S., Klein, P.S., Vetter, M.L., 2001. Regulation of eye development by frizzled signaling in *Xenopus*. Proc. Natl. Acad. Sci. U. S. A. 98, 3861–3866.
Reiss, J.O., Burd, G.D., 1997. Cellular and molecular interactions in the development of the *Xenopus* olfactory system. Semin. Cell Dev. Biol. 8, 171–179.
Ribisi Jr., S., Mariani, F.V., Aamar, E., Lamb, T.M., Frank, D., Harland, R.M., 2000. Ras-mediated FGF signaling is required for the formation of posterior but not anterior neural tissue in *Xenopus laevis*. Dev. Biol. 227, 183–196.
Richard-Parpaillon, L., Heligon, C., Chesnel, F., Boujard, D., Philpott, A., 2002. The IGF pathway regulates head formation by inhibiting Wnt signaling in *Xenopus*. Dev. Biol. 244, 407–417.
Rubenstein, J.L., Shimamura, K., Martinez, S., Puelles, L., 1998. Regionalization of the prosencephalic neural plate. Annu. Rev. Neurosci. 21, 445–477.
Saha, M.S., Servetnick, M., Grainger, R.M., 1992. Vertebrate eye development. Curr. Opin. Genet. Dev. 2, 582–588.
Sakaguchi, D.S., Janick, L.M., Reh, T.A., 1997. Basic fibroblast growth factor (FGF-2) induced transdifferentiation of retinal pigment epithelium: generation of retinal neurons and glia. Dev. Dyn. 209, 387–398.
Schlosser, G., Ahrens, K., 2004. Molecular anatomy of placode development in *Xenopus laevis*. Dev. Biol. 271, 439–466.
Schlosser, G., Northcutt, R.G., 2000. Development of neurogenic placodes in *Xenopus laevis*. J. Comp. Neurol. 418, 121–146.
Schulte-Merker, S., Smith, J.C., 1995. Mesoderm formation in response to Brachyury requires FGF signaling. Curr. Biol. 5, 62–67.
Shi, Y., Massague, J., 2003. Mechanisms of TGF-beta signaling from cell membrane to the nucleus. Cell 113, 685–700.
Stark, M.R., Biggs, J.J., Schoenwolf, G.C., Rao, M.S., 2000. Characterization of avian frizzled genes in cranial placode development. Mech. Dev. 93, 195–200.
Streit, A., Berliner, A.J., Papanayotou, C., Sirulnik, A., Stern, C.D., 2000. Initiation of neural induction by FGF signaling before gastrulation. Nature 406, 74–78.
Stump, R.J., Ang, S., Chen, Y., von Bahr, T., Lovicu, F.J., Pinson, K., de Iongh, R.U., Yamaguchi, T.P., Sassoon, D.A., McAvoy, J.W., 2003. A role for Wnt/beta-catenin signaling in lens epithelial differentiation. Dev. Biol. 259, 48–61.
Takabatake, T., Takahashi, T.C., Inoue, K., Ogawa, M., Takeshima, K., 1996. Activation of two Cynops genes, fork head and sonic hedgehog, in animal cap explants. Biochem. Biophys. Res. Commun. 218, 395–401.
Take-uchi, M., Clarke, J.D., Wilson, S.W., 2003. Hedgehog signaling maintains the optic stalk-retinal interface through the regulation of Vax gene activity. Development 130, 955–968.
Tamai, K., Semenov, M., Kato, Y., Spokony, R., Liu, C., Katsuyama, Y., Hess, F., Saint-Jeannet, J.P., He, X., 2000. LDL-receptor-related proteins in Wnt signal transduction. Nature 407, 530–535.
Tsang, M., Friesel, R., Kudoh, T., Dawid, I.B., 2002. Identification of Sef, a novel modulator of FGF signaling. Nat. Cell Biol. 4, 165–169.
Tsuda, H., Sasai, N., Matsuo-Takasaki, M., Sakuragi, M., Murakami, Y., Sasai, Y., 2002. Dorsalization of the neural tube by *Xenopus* tiarin, a novel patterning factor secreted by the flanking nonneural head ectoderm. Neuron 33, 515–528.
Twitty, V.C., 1930. Regulation in the growth of transplanted eyes. J. Exp. Zool. 55, 43–52.
van de Water, S., van de Wetering, M., Joore, J., Esseling, J., Bink, R., Clevers, H., Zivkovic, D., 2001. Ectopic Wnt signal determines the eyeless phenotype of zebrafish masterblind mutant. Development 128, 3877–3888.
Vendrell, V., Carnicero, E., Giraldez, F., Alonso, M.T., Schimmang, T., 2000. Induction of inner ear fate by FGF3. Development 127, 2011–2019.
Vogt, W., 1929. Gestaltungsanalyse am Amphibienkeim mit örtlicher Vitalfärbung. Roux's Arch. 120, 385–706.
Wang, S., Krinks, M., Lin, K., Luyten, F.P., Moos Jr., M., 1997a. Frzb, a secreted protein expressed in the Spemann organizer, binds and inhibits Wnt-8. Cell 88, 757–766.
Wang, S., Krinks, M., Moos Jr., M., 1997b. Frzb-1, an antagonist of Wnt-1 and Wnt-8, does not block signaling by Wnts-3A, -5A, or -11. Biochem. Biophys. Res. Commun. 236, 502–504.
Wawersik, S., Maas, R.L., 2000. Vertebrate eye development as modeled in *Drosophila*. Hum. Mol. Genet. 9, 917–925.
Wawersik, S., Purcell, P., Rauchman, M., Dudley, A.T., Robertson, E.J., Maas, R., 1999. BMP7 acts in murine lens placode development. Dev. Biol. 207, 176–188.
Wessely, O., De Robertis, E.M., 2002. Neural plate patterning by secreted signals. Neuron 33, 489–491.
Wessely, O., Agius, E., Oelgeschlager, M., Pera, E.M., De Robertis, E.M., 2001. Neural induction in the absence of mesoderm: beta-catenin-dependent expression of secreted BMP antagonists at the blastula stage in *Xenopus*. Dev. Biol. 234, 161–173.
Wilson, S.I., Rydstrom, A., Trimborn, T., Willert, K., Nusse, R., Jessell, T.M., Edlund, T., 2001. The status of Wnt signaling regulates neural and epidermal fates in the chick embryo. Nature 411, 325–330.
Woda, J.M., Pastagia, J., Mercola, M., Artinger, K.B., 2003. Dlx proteins position the neural plate border and determine adjacent cell fates. Development 130, 331–342.
Wurst, W., Bally-Cuif, L., 2001. Neural plate patterning: upstream and downstream of the isthmic organizer. Nat. Rev., Neurosci. 2, 99–108.
Yamamoto, Y., Jeffery, W.R., 2000. Central role for the lens in cave fish eye degeneration. Science 289, 631–633.
Yokotal, C., Mukasa, T., Higashi, M., Odaka, A., Muroya, K., Uchiyama, H., Eto, Y., Asashima, M., Momoi, T., 1995. Activin induces the expression of the *Xenopus* homologue of sonic hedgehog during mesoderm formation in *Xenopus* explants. Biochem. Biophys. Res. Commun. 207, 1–7.
Zhao, S., Hung, F.C., Colvin, J.S., White, A., Dai, W., Lovicu, F.J., Ornitz, D.M., Overbeek, P.A., 2001. Patterning the optic neuroepithelium by FGF signaling and Ras activation. Development 128, 5051–5060.
Zhou, X., Hollemann, T., Pieler, T., Gruss, P., 2000. Cloning and expression of xSix3, the *Xenopus* homologue of murine Six3. Mech. Dev. 91, 327–330.
Zuber, M.E., Perron, M., Philpott, A., Bang, A., Harris, W.A., 1999. Giant eyes in *Xenopus laevis* by overexpression of XOptx2. Cell 98, 341–352.
Zuber, M.E., Gestri, G., Viczian, A.S., Barsacchi, G., Harris, W.A., 2003. Specification of the vertebrate eye by a network of eye field transcription factors. Development 130, 5155–5167.
Zygar, C.A., Cook, T.L., Grainger Jr., R.M., 1998. Gene activation during early stages of lens induction in *Xenopus*. Development 125, 3509–3519.